UNIVERSIDADE ESTADUAL PAULISTA “JÚLIO DE MESQUITA FILHO”
INSTITUTO DE CIÊNCIA E TECNOLOGIA (ICT) –SÃO JOSÉ DOS CAMPOS

Relatório de Pós-Doutorado

José Roberto Amaro Mantovani

Hydrodynamic Flood Risk Mapping of the March 2024 Event in the Acre River Basin, Southwestern Amazon

São José dos Campos – SP
Setembro de 2025

PROGRAMA UNESP DE PÓS-DOUTORADO

Edital PROPG/PROPe 06/2024

Estagiário: José Roberto Amaro Mantovani

Endereço para acessar este CV: http://lattes.cnpq.br/6966987814678689

Supervisor: Enner Herenio de Alcântara

Endereço para acessar este CV: http://lattes.cnpq.br/7939379291404418

Title: Hydrodynamic Flood Risk Mapping of the March 2024 Event in the Acre River Basin, Southwestern Amazon.

Hydrodynamic Flood Risk Mapping of the March 2024 Event in the Acre River Basin, Southwestern Amazon.

Article submitted and awaiting review in the journal Modeling of Earth Systems and Environment (March 2025).

Abstract: Flood events have become increasingly frequent and severe in the southwestern Amazon, raising concerns about the capacity of urban areas to cope with intensifying hydroclimatic extremes. This study investigates the March 2024 flood in Rio Branco, Acre—one of the largest on record—by combining hydrometeorological time series analysis (1981–2024), two-dimensional hydrodynamic modeling using HEC-RAS, and spatial risk mapping. Rainfall and streamflow data did not exhibit statistically significant long-term trends; however, the recurrence and magnitude of extreme events, particularly those associated with La Niña conditions, indicate a shift toward more intense hydrological regimes. The simulation reproduced the observed flood dynamics with high accuracy and revealed that over 25% of the urban area is exposed to extreme flood hazard, with critical overlap in socially vulnerable neighborhoods. These results demonstrate the compounded nature of flood risk, driven by both climate variability and urban expansion into flood-prone zones. The study concludes that traditional assumptions about flood recurrence intervals are no longer sufficient for urban planning and that robust modeling and risk mapping must be integrated into climate adaptation strategies in Amazonian cities.

Keywords: flood risk, hydrodynamic modeling, Amazon Basin, Rio Branco, La Niña, climate extremes, spatial vulnerability.

Introduction

Global climate change has intensified in recent decades, triggering a wide range of environmental impacts that adversely affect the economy, agriculture, and both the physical and mental health of populations—particularly those who are socioeconomically disadvantaged. The increasing frequency and severity of extreme weather events such as heavy rainfall, hurricanes, and storms have posed significant challenges for urban planning and emergency management worldwide. These events often lead to severe flooding, causing devastating damage to infrastructure, communities, and local economies (Dunn et al. 2024).

According to the Emergency Events Database (https://www.emdat.be), climate change and extreme weather events have led to a substantial rise in disasters over the past 50 years. Natural hazards account for 50% of all recorded disasters, 45% of related fatalities, and 74% of total economic losses. More than 11,000 disasters have been attributed to climate-related events, resulting in over 2 million deaths and approximately USD 3.47 trillion in economic damages. Notably, over 91% of these deaths occurred in developing countries, and the average daily economic losses have increased sevenfold, from USD 49 million to USD 383 million over this period (IPCC 2022).

In Central and South America, floods constitute over 40% of all disaster events, according to the Intergovernmental Panel on Climate Change (IPCC 2023). In Brazil, the frequency of floods, flash floods, and urban inundation events has been steadily increasing. During the rainy season—typically from October to March—reports of such events are routine, especially when river discharge rises significantly and overflows riverbanks (Marengo et al. 2023). These hydrometeorological disasters are becoming more frequent and intense, posing a major challenge for numerous Brazilian municipalities and often resulting in irreversible losses for affected populations, largely driven by climate variability and change (IPCC 2023).

Assessing the risks associated with extreme events is a crucial step toward enabling evidence-based decision-making and effective disaster risk reduction by public authorities. Recent literature has increasingly focused on linking climate change to the occurrence of extreme events, aiming to understand their frequency, predictability, and associated risks, as well as to support compliance with environmental protocols. Notable studies in this field include Haidu et al. (2017), Vojtek et al. (2019), Kim et al. (2020), Muthusamy et al. (2021), Costabile et al. (2021), Rafiei-Sardooi et al. (2021), Tang et al. (2021), Zhao et al. (2023), Alcântara et al. (2023, 2024), Marengo et al. (2023, 2024), and Mantovani et al. (2023, 2024, 2025).

In this context, there is an urgent need for scientific research that supports concrete actions to mitigate the environmental and socio-economic impacts of climate change, particularly in vulnerable areas such as those examined in this study. Local governments must incorporate climate risk management into their sectoral and thematic public policies. Urban adaptation plans are required, and their actions must be aligned with national socio-economic development goals, regional inequality reduction strategies, and the United Nations Sustainable Development Goals (SDGs). The scientific challenge is not only to understand the phenomena but also to bridge the gap between available information and its application in decision-making processes. Identifying local susceptibilities and vulnerabilities, and addressing them through appropriate planning and management, is essential.

According to the Amazon Protection System (SIPAM), in 2024, the city of Rio Branco—the capital of Acre state in the Western Brazilian Amazon—experienced the second-largest flood in its recorded history, which dates back to 1971. The highest river level recorded in 2024 was 17.89 meters on March 6, as reported by the Rio Branco Civil Defense. The highest historical flood level remains 18.40 meters, recorded in March 2015. More than 70,000 people were directly or indirectly affected by the 2024 flood. A total of 51 neighborhoods and 23 rural communities were inundated, displacing over 4,000 individuals, according to the municipal government. These data underscore the reality that climate change is not a distant concern but an ongoing process with tangible consequences in Brazil and worldwide. Thus, the present study aims to systematically analyze and model the March 6, 2024 flood event in Rio Branco, Acre, to better understand the dynamics of such events and to inform future mitigation strategies.

Description of the study area

Rio Branco is the capital of the state of Acre, located in the Northern Region of Brazil. Situated along the banks of the Acre River (Fig. 1), the city serves as the state's main financial, administrative, political, and cultural hub. It is also the westernmost state capital in Brazil, lying approximately 3,030 kilometers from Brasília, the federal capital.

The municipality spans a total area of 8,834.942 km², making it the fifth-largest municipality in Acre in terms of territorial extent. Of this area, approximately 44.96 km² correspond to the urban perimeter, ranking Rio Branco as the 62nd largest city in Brazil by urban area. According to the most recent demographic census conducted by the Brazilian Institute of Geography and Statistics (IBGE 2023), the city has a population of 364,756, making it the seventh most populous city in the Northern Region of Brazil.

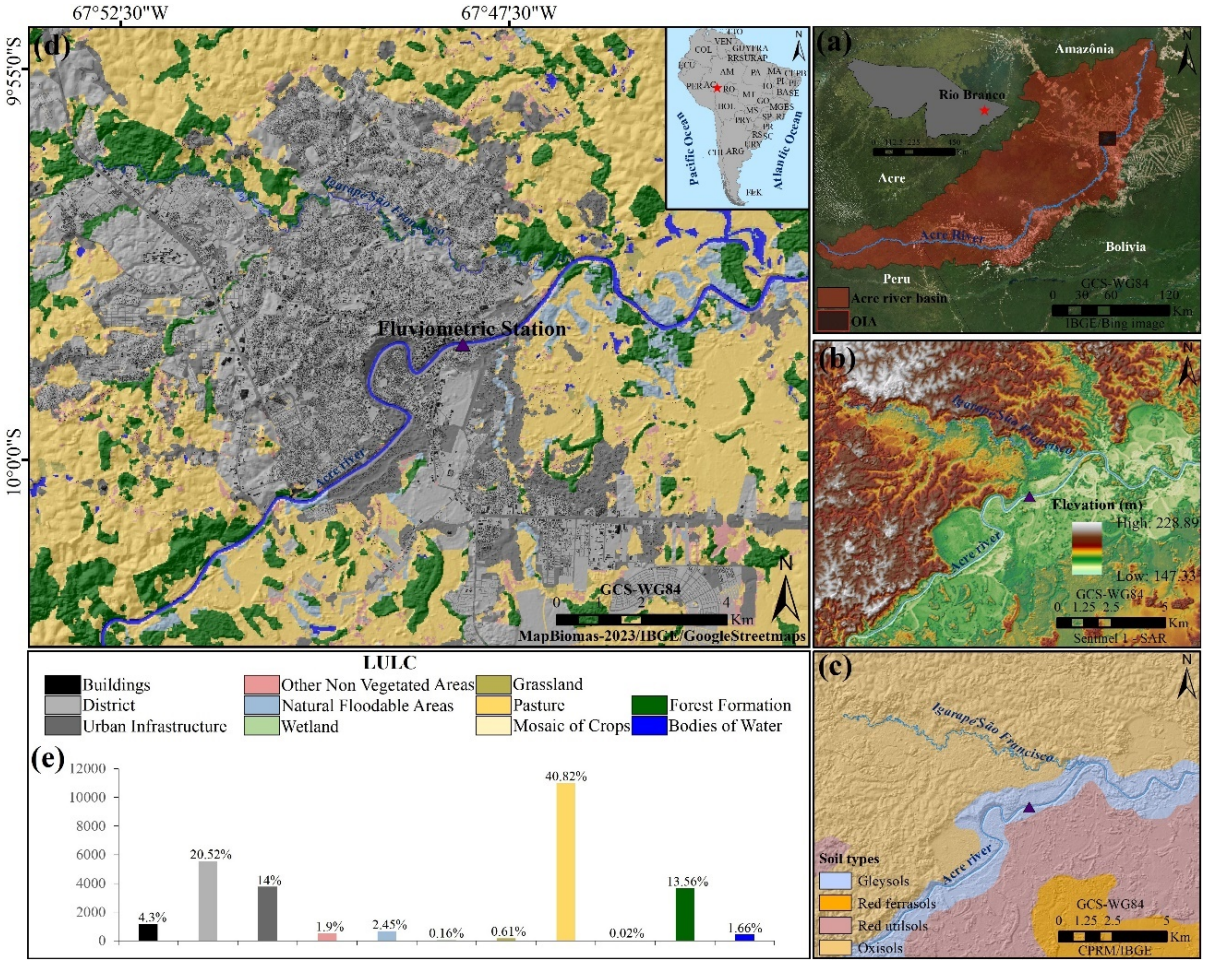

Fig 1. (a) Location of study site in Brazil, highlighting the Acre River basin and Capital of the state of Acre; (b) Digital Elevation Model (MDE) for the study area with drainage network; (c) Soil Types; (d) land use and land cover for Rio Branco (Acre State, Brazil); (e) land use and land cover (LULC) area in ha and in %.

Geologically, Rio Branco is predominantly composed of sedimentary rocks, with a dominance of sandstones, and is almost entirely covered by floodplain formations. The region's climate is classified as equatorial, characterized by consistently high temperatures and elevated humidity levels throughout the year. The rainy season typically extends from September to May and coincides with what is locally referred to as "winter," despite the continued presence of high temperatures. In contrast, the dry season—commonly called "summer"—occurs between June and August. Acre is among the Brazilian states with the highest annual rainfall, with precipitation levels exceeding 2,100 millimeters (Nimer 1977).

Methodology and data used

Methodology flowchart

The research process was conducted in the following steps (Fig. 2), a comprehensive flow diagram outlining the methodology used to map the flood extent, assess flood risk, and determine hazard ratings (i.e., risk to people) within the designated study area.

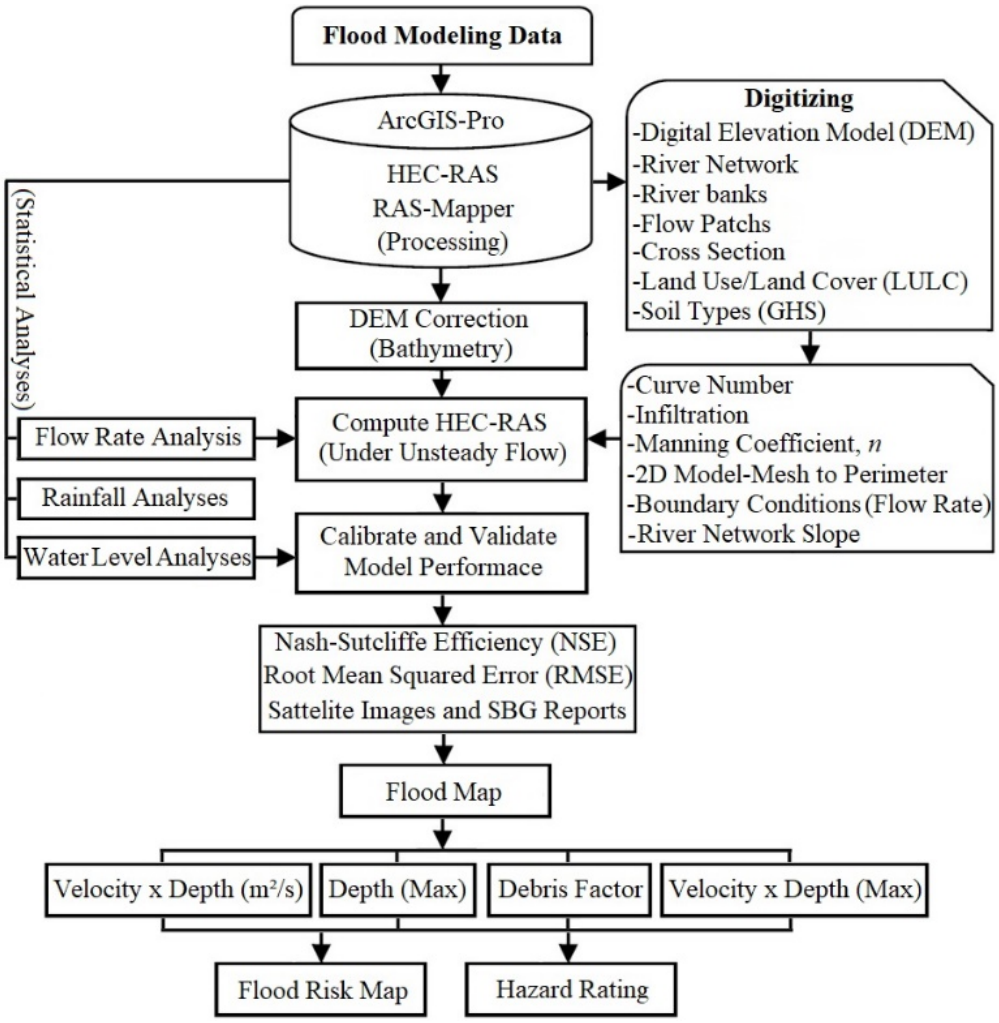

Fig 2. Conceptual flow diagram illustrating the methodological framework for flood mapping, risk assessment, and hazard classification applied in this study.

Data used

A wide range of data sources was utilized in this study, encompassing fluviometric, rainfall, thematic, remote sensing, and census datasets. Each dataset represents a key environmental or socioeconomic variable essential for accurately mapping the flood event and evaluating associated risks in Table 1. These datasets include information on topographic and physiographic features, hydrodynamic components, land use and land cover (LULC), meteorological conditions, and population distribution—collectively providing a comprehensive representation of the study area's environmental and social context.

Table 1. Description of environmental and socioeconomic variables used in the development of the flood susceptibility assessment.

Database	Processing	Data Source
Sentinel 1–SAR	Elevation (m)	https://panda.copernicus.eu/web/cds-catalogue/panda
	Shaded Relief	
CHIRPS	Rainfall time series	https://app.climateengine.org/climateEngine

		http://ftp.cptec.inpe.br/modelos/tempo/MERGE/
Thematics	Soil types	https://www.sgb.gov.br
	Land Use and Land Cover	https://code.earthengine.google.com/?accept_repo=users%2Fmapbiomas%2Fuser-
Fluviometrics	Flow Rate (m^3/s)	https://www.snirh.gov.br/hidroweb/serieshistoricas
	River Level (m)	
Sentinel 2 – MSI	False color imagery	https://panda.copernicus.eu
Cartographic	Drainage Network	https://www.ibge.gov.br/geociencias/downloads http://download.geofabrik.de
	Urban Infrastructure	
	Districts	
	Buildings	
	Census Sectors	

To develop the Digital Elevation Model (DEM), a high-resolution C-band Synthetic Aperture Radar (SAR) image from the Sentinel-1 satellite was utilized (product ID: S1A_IW_GRDH_1SDV_20230823T100632_20230823T100659_050001_0603F5_DC53), featuring a spatial resolution of 10 meters. Complementary multispectral data from the MSI (Multispectral Instrument) sensor onboard Sentinel-2 were employed to capture the land surface conditions before and after the flood event. Specifically, pre-event imagery (S2A_MSIL2A_20240215...) and post-event imagery (S2B_MSIL2A_20240311...)—both at 10-meter resolution—were used to support spatial analysis and validate the results obtained from the hydraulic simulation.

Hydrological data, including river stage and discharge, were sourced from the National Water and Sanitation Agency (ANA) via the HIDROWEB platform, using data from station code 13600002 located in Rio Branco, Acre. For precipitation analysis, the study relied on the Climate Hazards Group InfraRed Precipitation with Station data (CHIRPS), as described by Funk et al. (2015). CHIRPS integrates satellite imagery with ground-based station observations to provide precipitation estimates at daily, monthly, and annual scales, with a spatial resolution of 0.05° × 0.05°. The dataset covers the period from January 1985 through December 2024.

Land use and land cover (LULC) information was obtained from the MapBiomas Project, Collection 9, which provides classified land cover data at a spatial resolution of 30 meters. Urban infrastructure data were retrieved from OpenStreetMap in shapefile format. Additionally, census sector shapefiles were used to distinguish zones of varying population density within the urban area. Soil classification data, published at a scale of 1:800,000, were incorporated to derive surface runoff and infiltration maps, which were essential for parameterizing and calibrating the two-dimensional hydraulic flood model.

Digital Elevation Model Processing

A major challenge in hydraulic modeling is the frequent unavailability of bathymetric data within terrain datasets. Accurate representation of surface elevations—especially within river channels and adjacent floodplains—is critical for developing reliable hydraulic models (Mantovani et al. 2024). An effective terrain model must capture key morphological features that influence water flow, including channel beds, banks, and elevated structures such as levees and roads (USACE 2010).

The DEM initially derived from Sentinel-1 SAR imagery, with a spatial resolution of 10 meters, lacked bathymetric detail within the river channel. To address this, the DEM was corrected and enhanced by incorporating bathymetric information obtained from the fluviometric station maintained by ANA (station code 13600002, Acre River, Rio Branco) and from geological reports published by the Geological Survey of Brazil (*Serviço Geológico do Brasil*, formerly CPRM, current SBG).

A one-dimensional (1D) hydraulic representation of the channel was developed by defining the river centerline, cross-sections, and bank lines. These features were integrated and interpolated using RAS Mapper (USACE 2010) to generate a continuous surface representing the riverbed profile. The resulting modified DEM was constructed by combining this interpolated channel surface—assigned maximum elevation priority—with the radar-derived terrain model (Hosseini et al. 2006; Al-Zahrani 2017), thus producing a more hydrodynamically realistic elevation model for subsequent flood simulation.

Flood Inundation Modeling

All datasets were processed and organized within the HEC-RAS (Hydrologic Engineering Center – River Analysis System) environment, using the RAS Mapper platform for spatial integration and hydraulic modeling (USACE 2010).

In this study, flood simulation was conducted using the **unsteady flow method**, which allows for the dynamic reconstruction of the flood event that occurred on **March 6, 2024**. Under the unsteady flow approach, boundary conditions are defined by assigning a discharge hydrograph at the upstream boundary and a stage-discharge rating curve at the downstream boundary. For relatively short channel reaches, the kinematic wave approximation—where discharge remains constant along the flow path—is often preferred over the dynamic wave approach, which accounts for attenuation and backwater effects (USACE 2010).

The main input parameters for the two-dimensional (2D) model included channel topography, computational mesh, boundary conditions (based on discharge data for the main channel and the tributary *Igarapé São Francisco*; Fig 1c), an outflow condition, and the Manning's roughness coefficient (n). The boundary conditions used to simulate the event were based on daily discharge records from February 21 to March 18, 2024.

The HEC-RAS 2D framework represents a state-of-the-art tool for flood modeling, as it incorporates both vertical and horizontal components of the flood wave, enabling more accurate simulation of flood extents, depths, velocities, and other hydrodynamic variables (Mantovani et al. 2025). Compared to traditional one-dimensional models, the 2D approach enhances the resolution and physical realism of simulations, especially in complex urban and floodplain environments.

Key input layers for the 2D model included the corrected Digital Elevation Model (DEM), land use and land cover (LULC), and reclassified soil types grouped into hydrologic soil classes (Table 2). The LULC and soil maps were used to assign surface roughness values (Manning's n) used values proposed by Davis and Sorensen 1969 and to define infiltration and runoff parameters based on the Curve Number (CN) method, developed by the Natural Resources Conservation Service (Formerly the Soil Conservation Service).

Table 2. Manning's n roughness coefficients by land cover class, associated Curve Number (CN) values by hydrologic soil group (HSG), and minimum infiltration rates used for hydrological modeling.

Decription	**LULC**	**Manning's *n***	**Curve-Number (GHS)**			**Abstraction Ratio**	**Minimum Infiltration Rate (mm/hr)**
			A	**C**	**D**	0.2	0.12
Forest	Forest	0.06	26	58	61	0.1	0.12
Non-Forest Natural	Grassland	0.04	49	84	89	0.1	0.12
	Wetland	0.045	90	94	98	0.1	0.12
Farming	Pasture	0.04	39	74	80	0.1	0.12
	Mosaic of Crops		39	75	83	0.1	0.12
Non-vegetated area	Buildings	0.07	91	95	97	0.1	0.12
	Districts		72	82	85	0.1	0.12
	Urban Infrastructure		77	90	92	0.1	0.12
Water	Bodies of Water	0.035	100	100	100	0	0
	Natural Floodable Areas		98	98	98	0	0

The unsteady flow method was applied using a discharge hydrograph at the upstream boundary and a stage–discharge relationship at the downstream boundary. In typical short

channel reach simulations, the kinematic wave assumption—which maintains constant discharge—is often preferred over the dynamic wave, which accounts for discharge attenuation (Ponce and Lugo 2001).

For the simulation of the March 2024 flood event, boundary conditions were defined using daily discharge data from the main channel (Acre River) spanning February 21 to March 18, 2024. In the case of the tributary Igarapé São Francisco, where discharge data were unavailable, the channel slope was used as a boundary condition, based on the energy grade line calculated from bed slope measurements.

In river reaches lacking fluviometric data, the "Normal Depth" boundary condition is a widely used alternative (USACE 2010). This method, which closely resembles the Modified Puls routing technique, assumes that storage within a reach is primarily governed by outflow. It automatically derives storage–discharge relationships based on Manning's equation, the normal depth assumption, and user-defined channel geometry. While this approach simplifies parameterization and enhances computational efficiency, it does not account for backwater effects or the influence of hydraulic structures, as it bypasses full hydraulic simulation.

Model Performance Evaluation

To calibrate and validate the model and for comparison purposes, quantitative information is required to measure model performance. In this study, to validate and assess the results generated with the model, we used observed data from river levels extracted from the fluviometric station and data generated with the model. The selected period consisted of 1 day after the event (06 March 2024), from the 07nd to the 18th march 2024; during and after calibration, we used two statistical indicators to evaluate the existence of systematic errors: the Nash–Sutcliffe efficiency (NSE) and the RMSE-observations standard deviation ratio (RSR). The Nash–Sutcliffe efficiency (NSE) is used to assess the predictive skill of hydrological models. It consists of a normalized statistic that determines the relative magnitude of the residual variance ("noise") compared to the measured data variance ("information") (Nash and Sutcliffe 1970). The NSE indicates how well the plot of observed versus simulated data fits the 1:1 line. It is defined as Equation 1:

$$NSE = 1 - \frac{\sum_{t=1}^{T}(Q_0^t - Q_m^t)^2}{\sum_{t=1}^{T}(Q_0^t - \overline{Q_0})^2} \quad \textbf{Eq.1}$$

where (*Q0*) is the mean of observed discharges, and *Qm* is modeled discharge. *Qt0* is observed discharge at time *t*.

The Nash–Sutcliffe efficiency (NSE) is calculated as 1 minus the ratio of the error variance of the modeled time series to the variance of the observed time series. An NSE of 1 indicates a perfect model, while an NSE of 0 means the model is no better than the mean of the time series in terms of prediction. Negative NSE values indicate that the observed mean is a better predictor than the model. NSE values closer to 1 suggest greater predictive skill of the model. Different authors have proposed NSE values as thresholds of sufficiency. Subjective application of different NSE values as thresholds of sufficiency have been suggested by several authors (Ritter and Muñoz-Carpena 2013; McCuen 2006; Moriasi et al. 2007). The root-mean-square deviation (RMSD) measures the average size of discrepancies between predicted and observed values. It is used to assess the accuracy of forecasting models within a dataset. RMSD is always non-negative, with lower values indicating better accuracy. However, it is important to note that RMSD comparisons between datasets are unreliable due to its scale dependency (Hyndman and Koehler 2006). The RMSE-observations standard deviation ratio (RSR) is determined by dividing the RMSE by the standard deviation of the measured data. The RSR ranges from an optimal value of 0 to a higher positive value. A lower RSR corresponds to a lower RMSE and indicates better performance in model simulation. The RSR standardizes the root-mean-square Error (RMSE) by incorporating the standard deviation of observed values. It goes from an optimal value of 0 to infinity. Based on the RSR, Moriasi et al. (2007) indicates performance ratings as follows: (i) very-good (0–0.50); (ii) good (0.50–0.60); (iii) satisfactory (0.60–0.70); or(iv) unsatisfactory (>0.70). It is defined as Equation 2:

$$RSR = \frac{1}{n}\sum_{i=1}^{n}(P_i - Q_i)^2 \qquad \textbf{Eq. 2}$$

where *Pi* is the predicted value and *Oi* is the observed value.

Flood risk mapping

To assess flood risk, we employed the methodology outlined by the U.S. Federal Emergency Management Agency (FEMA 2018). This method categorizes risk levels into five distinct categories: low, moderate, high, very high, and extreme detail in Table 3. The approach was utilized (Beden and Keskin 2021) to generate a flood map and evaluate flood risks in scenarios where flow data in Turkey were insufficient. This method utilizes velocity and flood depth data derived from the 2D HEC-RAS model.

Table 3. Flood risk classifications scheme.

Velocity x Depth (m^2/s)	Flood Risk
< 0.2	Low
0.2 – 0.5	Moderate
0.5 – 1.5	High
1.5 – 2.5	Very High
> 2.5	Extreme

Hazard rating (risk to people*)*

The "hazard rating" or "risk to people" is a measure used to assess and categorize the likelihood and severity of a specific risk that may affect people's safety. This rating system is commonly used in various fields, such as occupational health and safety, disaster management, engineering, and environmental security (Mantovani et al. 2025). During floods, individuals frequently face higher risks of injury and death due to their actions. Many do not realize the power of the water flow and endanger both themselves and others by venturing into floodways. The guide on assessing risks to individuals suggests utilizing the hazard rating approach outlined to determine the degree of flood hazard in Equation 3:

$$HR = d(v + n) + DF \qquad \textbf{Eq. 3}$$

where (d) is maximum flood depth (m), v is maximum flood velocity (m/s). DF (debris factor); 0: negligible debris; 0.5: moderate debris and 1: high debris (urban areas, forests).

The hazard rating system, as detailed in Equation 3, incorporates various factors to assess flood risk. These factors include flood depth (d in meters), flow velocity (v in meters per second), the debris factor (DF), and a constant value represented by 'n' set at 0.5 (36,37). The appropriate debris factors corresponding to different flood depths, velocities, and dominant land use are listed in Table 4.

Table 4 Debris factor (DF) selection.

Velocity x Depth	Farming	Forest	Urban
0.00 – 0.25 m	0	0	0
0.25 – 0.75 m	0	0.5	1
d>0.75 m and/or v>2	0.5	1	1

The level of flood hazard is then determined based on predefined intervals provided in Table 5.

Table 5 Flood hazard levels

Thresholds for Flood Hazard Rating	Flood Hazard Level	Description
<0.75	Low	Caution: flood zone with shallow flowing water or deep standing water
0.75-1.25	Moderate	Dangerous for some: flood zone with deep or fast flowing water
1.25-2.5	Significant	Dangerous for most people: flood zone with fast flowing water
>2.5	Extreme	Dangerous for all: flood zone with deep, fast flowing water

The integration of multiple data sources—both iconographic (e.g., satellite imagery) and cartographic (e.g., spatial vector layers)—enables a comprehensive assessment of the impacts of extreme precipitation events on flood dynamics. This multidisciplinary approach supports both qualitative and quantitative analyses, enhances the evaluation of model accuracy, and facilitates the identification of flood-prone, vulnerable, and high-risk areas.

Following the calibration and validation of the hydrodynamic model, the results were analyzed through both statistical and spatial methods. Flood risk maps were generated using ArcGIS Pro, along with supporting graphics and thematic layers, to visualize flood extent, depth, and associated risk levels with high spatial resolution.

Climate, Hydrology Analyses in Rio Branco, Acre, in March 2024

Figure 3 displays a boxplot illustrating the distribution of daily river level measurements for each year between 1981 and 2024. Each box represents the interquartile range (IQR), encompassing the middle 50% of daily water level values—from the 25th to the 75th percentile—within a given year. The horizontal line inside each box denotes the median, providing a robust measure of central tendency that is less influenced by outliers.

The whiskers extend to the smallest and largest values that lie within 1.5 times the IQR from the lower and upper quartiles, respectively. Observations beyond this range are plotted as individual points, indicating hydrological outliers. End caps at both whisker limits visually define the boundaries of typical variation.

Mean river levels are marked with black circular symbols, serving as an additional measure of central tendency to complement the medians. The plot reveals considerable interannual variability, with certain years—particularly in the mid-2010s—exhibiting wider IQRs and more frequent outliers, suggesting increased occurrences of hydrological extremes such as floods or droughts. In contrast, narrower IQRs observed in the early 2000s reflect more stable hydrological conditions.

A visual analysis suggests a slight downward trend in both median and mean values over the study period, consistent with the results of the temporal trend analysis indicating a gradual decline in average river levels.

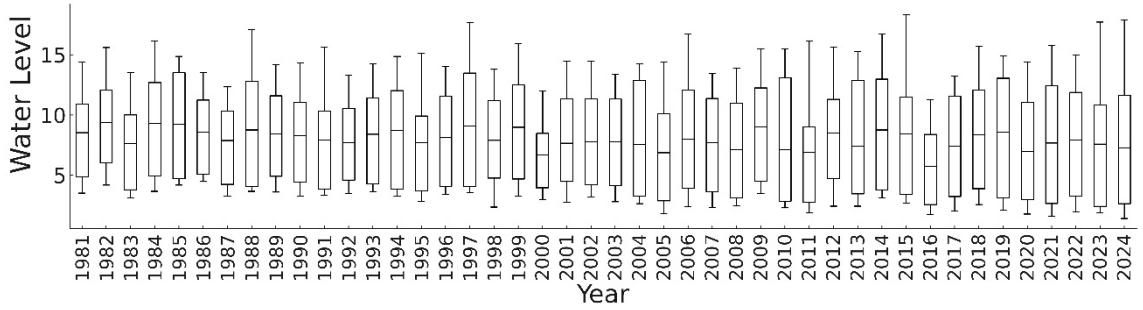

Fig 3. Boxplot showing the distribution of daily river levels for each year from 1981 to 2024. The plot highlights interannual variability, median and mean values, and extreme hydrological events.

The temporal trend analysis revealed a statistically significant decline in annual mean river levels throughout the study period (1981–2024), with a slope of –0.0301 meters per year (p-value = 0.0101; R^2 = 0.2455). This negative trend suggests a gradual reduction in water levels over the decades. Although the trend is statistically significant, the moderate coefficient of determination indicates that a substantial portion of the variability is explained by other environmental or anthropogenic factors beyond time alone. Such results highlight the complexity of hydrological systems in tropical watersheds, which are often modulated by climatic drivers such as ENSO phases, local precipitation regimes, and land use dynamics.

Interannual variability further reinforces this complexity. The largest annual rise in average water level occurred between 2016 and 2018 (+2.63 m), while the most severe drop was observed between 2015 and 2016 (–3.19 m), underscoring the influence of extreme hydrological events. These abrupt changes may reflect the impacts of anomalous rainfall, changes in watershed infiltration capacity, or infrastructure-related effects on flow regulation. Extreme value analysis revealed a historical maximum river level of 28.39 meters on November 20, 2023, and a minimum of –0.52 meters on March 22, 2021. These observations serve as critical hydrological thresholds for flood and drought risk assessments, respectively.

Seasonal behavior is also evident in the river level dynamics. July exhibited the highest average monthly water level (8.96 m), whereas March recorded the lowest (5.29 m), aligning with the typical seasonal precipitation and evapotranspiration patterns in the western Amazon basin. This clear seasonality is consistent with the regional climatic regime, characterized by a pronounced wet season from October to May and a drier interval during the austral winter months.

Additionally, a structural break analysis detected a significant change in the behavior of river levels around 2016. This inflection point may be attributed to changes in climatic forcing, intensified land use alterations, or modifications in hydrological regulation mechanisms across the basin. Decadal comparisons further support the long-term declining trend: the 1980s registered the highest average river levels (8.71 m), while the 2020s—up to 2024—recorded the lowest (6.27 m). Such decadal-scale declines, combined with increasing variability, may reflect ongoing environmental degradation, deforestation, or broader climatic shifts affecting hydrological balance in the region.

The average annual standard deviation of river levels was approximately 2.92 meters, underscoring substantial interannual fluctuations. This variability is particularly relevant in the context of risk mapping, as it reflects the basin's exposure to both flood and drought extremes, requiring adaptive management strategies and robust early warning systems.

Table 6. Summary of river level time series analysis (1981–2024), including trend statistics, annual variations, historical extremes, seasonal behavior, structural break, decadal averages, and interannual variability.

Analysis	Main Result
Temporal Trend (Slope)	-0.0301 m/year
Temporal Trend (R^2)	0.2455
Temporal Trend (p-value)	0.0101
Largest Annual Increase	2016 ➔ 2018 (+2.63 m)
Largest Annual Decrease	2015 ➔ 2016 (-3.19 m)
Historical Maximum (Date and Level)	2015-01-03 (18.35 m)
Historical Minimum (Date and Level)	2016-01-08 (1.72 m)
Month with Highest Average Level	1 (Average 8.18 m)
Month with Lowest Average Level	1 (Average 8.18 m)
Year of Detected Structural Break	2008
Decade with Highest Average Level	1970s (Average 9.47 m)
Decade with Lowest Average Level	2020s (Average 7.50 m)
Average Annual Variability (Standard Deviation)	4.51 m

Figure 4 presents a boxplot depicting the distribution of daily rainfall values for each year from 1981 to 2024. Each box illustrates the interquartile range (IQR), encompassing the central 50% of rainfall observations—bounded by the 25th and 75th percentiles. The horizontal red line within each box represents the median, offering a robust indicator of central tendency that is less influenced by outliers or extreme values. Black circular markers denote the annual mean rainfall, enabling a comparative assessment between mean and median values, and revealing the symmetry or skewness of the data distribution.

The whiskers extend to the smallest and largest values within 1.5 times the IQR, while data points beyond this range are plotted as outliers, indicating extreme daily precipitation events. The inclusion of top and bottom caps helps visually constrain the main range of variability, clearly demarcating the typical boundaries of rainfall behavior in each year.

Notably, the plot reveals pronounced interannual variability in rainfall patterns. Certain years exhibit wider interquartile ranges and a higher number of outliers, suggesting highly variable rainfall conditions and an increased frequency of extreme precipitation events—factors that are critical in flood modeling and hydrological risk assessment. In contrast, years with narrower boxes and fewer outliers reflect more stable and consistent rainfall regimes, potentially associated with regular seasonal cycles.

Importantly, no clear long-term trend is visually apparent in the boxplot, either in medians or means. This observation is consistent with the temporal trend analysis, which indicated a statistically non-significant slope. Nonetheless, the widespread presence of outliers across several years emphasizes the recurrence of extreme rainfall events throughout the period analyzed—events that play a crucial role in shaping flood dynamics and hazard exposure in the region.

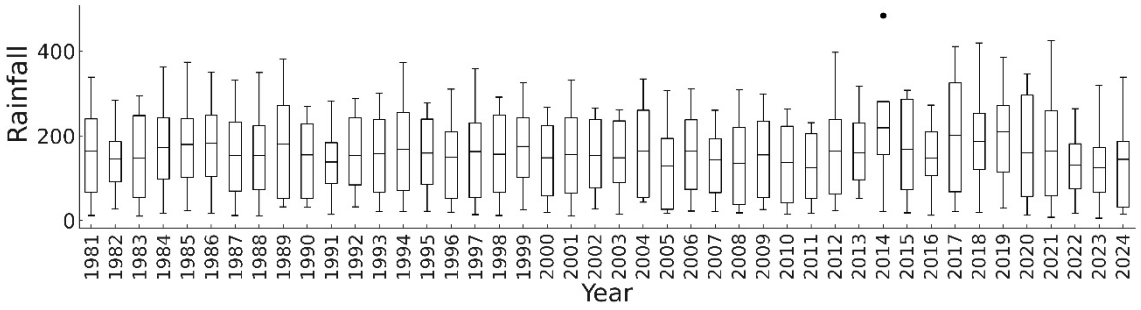

Fig 4. Boxplot showing the distribution of daily rainfall values for each year from 1981 to 2024. The plot illustrates interannual variability, median and mean values, and the frequency of extreme precipitation events.

The temporal trend analysis revealed a very slight and statistically non-significant increase in annual mean rainfall over the period from 1981 to 2024. The estimated slope was +0.0454 mm/year (p-value = 0.8710; R^2 = 0.0011), indicating that there is no substantial long-term trend in rainfall accumulation for the region. The extremely low R^2 value suggests that annual rainfall variability is largely influenced by non-temporal factors, such as atmospheric circulation patterns, land-atmosphere interactions, or localized climatic anomalies, rather than a progressive increase or decrease over time.

Interannual variability remains a defining feature of the precipitation regime in the study area. The most notable annual increase occurred between 2023 and 2025, with a rise of +103.37 mm, whereas the most significant annual decline took place between 2009 and 2011, amounting to –29.54 mm. These variations reflect the inherent natural fluctuation of rainfall on shorter timescales, possibly modulated by regional phenomena such as the South American Monsoon System or El Niño/La Niña events. Extreme daily rainfall values further highlight the system's volatility, with the highest recorded on February 15, 1992, reaching 639.12 mm. Conversely, days with no measurable rainfall (0.00 mm) occurred multiple times throughout the series, underscoring the alternation between wet extremes and dry spells.

Seasonal dynamics were also clearly evident. January was identified as the wettest month, with an average rainfall of 11.22 mm/day, while August was the driest, with a mean of 4.62 mm/day. This pattern aligns with the regional bimodal rainfall regime of the western Amazon, driven by the migration of the Intertropical Convergence Zone (ITCZ) and the onset of the dry season during the austral winter.

Although a structural break was detected around the year 2023, its significance is unclear due to the absence of a consistent trend in the long-term data. The shift may reflect a temporary anomaly rather than a fundamental change in rainfall regime. Decadal comparisons support this interpretation: the 1980s registered the highest average rainfall (10.62 mm/day), whereas the 2020s (through 2024) recorded the lowest (8.40 mm/day), suggesting a modest but noticeable decline that warrants further investigation using complementary climate diagnostics such as sea surface temperature anomalies or land use change metrics.

The average interannual variability, measured by the standard deviation of annual mean rainfall, was approximately 8.35 mm. This relatively high value reinforces the need to account for strong year-to-year fluctuations in water availability, which have direct implications for flood risk, drought vulnerability, and regional water resource planning.

Table 7. Summary of rainfall time series analysis (1981–2024), including trend statistics, annual variations, historical extremes, seasonal patterns, structural break, decadal averages, and interannual variability.

Analysis	Main Result
Temporal Trend (Slope)	0.0454 mm/year
Temporal Trend (R^2)	0.0011
Temporal Trend (p-value)	0.8710
Largest Annual Increase	2023 ➔ 2025 (+103.37 mm)
Largest Annual Decrease	2009 ➔ 2011 (-29.54 mm)
Historical Maximum (Date and Rainfall)	2015-01-05 (425.21 mm)
Historical Minimum (Date and Rainfall)	2023-01-07 (5.79 mm)
Month with Highest Average Rainfall	1 (Average 158.44 mm)
Month with Lowest Average Rainfall	1 (Average 158.44 mm)
Year of Detected Structural Break	2023
Decade with Highest Average Rainfall	2010s (Average 163.37 mm)
Decade with Lowest Average Rainfall	2020s (Average 143.56 mm)
Average Annual Variability (Standard Deviation)	100.55 mm

Figure 5 presents a boxplot illustrating the distribution of daily river flow rates, measured in cubic meters per second, for each year between 1981 and 2024. Each box represents the interquartile range (IQR), which captures the central 50% of flow values—bounded by the 25th and 75th percentiles. The horizontal red line within each box indicates the median, offering a robust measure of central tendency that is relatively unaffected by extreme values. Black circular markers denote the annual mean flow rate, enabling visual comparison between the mean and median to evaluate the skewness of the data distribution.

The whiskers extend to values within 1.5 times the IQR beyond the lower and upper quartiles, and caps mark these endpoints to delineate the typical range of variability. Observations that fall outside this range are plotted as individual points, reflecting outliers that correspond to extreme hydrological events, such as major floods. In years where a significant divergence is observed between mean and median flow rates, this suggests a skewed distribution—often driven by high-magnitude flood events.

Marked interannual variability is evident across the time series. Several years show wide interquartile ranges and numerous outliers, indicating periods of intense hydrological fluctuation, possibly linked to climatic anomalies or changes in watershed conditions. Conversely, years with narrower boxes and fewer outliers represent periods of greater flow stability, potentially associated with more regular precipitation and runoff dynamics.

No clear upward or downward trend is visually apparent in the medians across the series, a pattern consistent with the statistical results of the trend analysis, which indicated a non-significant slope. Despite the absence of a long-term trend, the presence of very high flow rates in specific years highlights the need for sustained hydrological monitoring and the implementation of early warning systems to anticipate flood-related hazards.

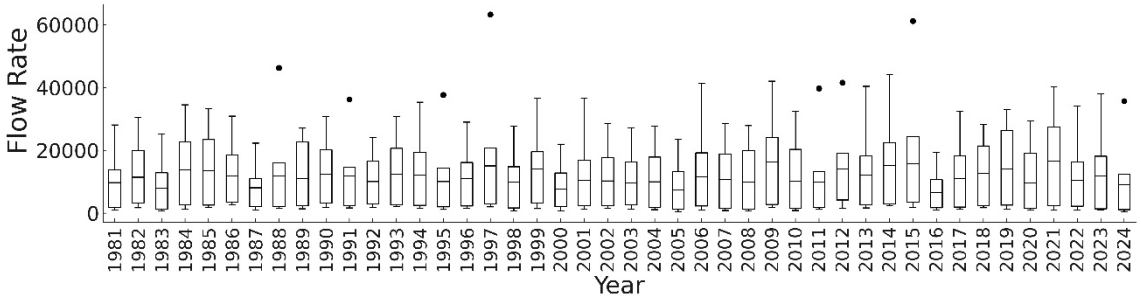

Fig 5. Boxplot showing the distribution of daily river flow rates (m^3/s) for each year from 1981 to 2024. The figure highlights interannual variability, central tendencies, and the occurrence of extreme discharge events.

The temporal trend analysis indicated a very slight decline in the annual mean river flow rate over the period from 1981 to 2024, with a slope of –4.8743 m^3/s per year (p-value = 0.8845; R^2 = 0.0009). Despite the negative slope, the trend is statistically non-significant, suggesting that no consistent long-term increase or decrease in average discharge occurred during the study period. The extremely low R^2 value reinforces the notion that the annual variability in flow rates is largely driven by factors other than time, such as precipitation extremes, soil moisture dynamics, vegetation cover, or human interventions in the watershed.

Significant interannual variation is evident in the dataset. The largest year-to-year increase in average flow rate occurred between 2008 and 2009, with a jump of +6,329.75 m^3/s. In contrast, the most pronounced decline took place between 2015 and 2016, when the mean flow dropped by –7,745.02 m^3/s. These sharp fluctuations are indicative of extreme hydrological conditions and likely reflect the influence of intense rainfall, droughts, or abrupt climatic shifts such as those associated with El Niño or La Niña phases.

Extreme value analysis further emphasized this volatility: the highest daily flow rate during the study period was recorded on February 15, 1992, at 16,271.20 m^3/s. On the other end of the spectrum, several days registered flow rates of 0.00 m^3/s, representing complete flow cessation, which may be linked to seasonal drying patterns or upstream management actions such as dam operation or water diversion.

Seasonal patterns were also evident in the discharge data. July recorded the highest average monthly flow rate (2,731.85 m³/s), typically following peak rainfall periods. August, by contrast, showed the lowest average flow (1,765.62 m³/s), consistent with the seasonal decline in precipitation and increased evapotranspiration during the dry season. These monthly dynamics align well with the regional hydrological cycle observed in the western Amazon.

A structural break analysis identified a potential shift in flow regime around the year 2009. This coincides with one of the largest observed changes in discharge and may indicate a transition in the basin's hydrological response. Such a shift could be linked to climate anomalies, large-scale deforestation, land use changes, or modifications in water regulation infrastructure.

Decadal comparisons reinforce the perception of a gradual decline in river flow. The 1980s exhibited the highest average flow rate (2,845.92 m³/s), while the 2020s (up to 2024) had the lowest (2,164.80 m³/s). This downward tendency, though subtle, suggests long-term changes in hydrological processes that warrant closer investigation. The interannual variability remains high, with a standard deviation of 1,205.32 m³/s, underscoring the dynamic nature of river discharge in the region and the need for adaptive water management strategies.

Table 8. Summary of river flow rate time series analysis (1981–2024), including trend statistics, interannual variations, historical extremes, seasonal behavior, structural break, decadal averages, and discharge variability.

Analysis	Main Result
Temporal Trend (Slope)	-4.8743 m³/s per year
Temporal Trend (R^2)	0.0009
Temporal Trend (p-value)	0.8845
Largest Annual Increase	2008 ➔ 2009 (+6329.75 m³/s)
Largest Annual Decrease	2015 ➔ 2016 (-7745.02 m³/s)
Historical Maximum (Date and Flow Rate)	1997-01-03 (63292.00 m³/s)
Historical Minimum (Date and Flow Rate)	2015-01-01 (364.99 m³/s)
Month with Highest Average Flow Rate	1 (Average 12103.48 m³/s)
Month with Lowest Average Flow Rate	1 (Average 12103.48 m³/s)
Year of Detected Structural Break	1983
Decade with Highest Average Flow Rate	1970s (Average 13859.91 m³/s)
Decade with Lowest Average Flow Rate	1980s (Average 10213.42 m³/s)
Average Annual Variability (Standard Deviation)	11327.13 m³/s

Figure 6 presents a boxplot of daily river flow and water level values from February 21 to March 18, 2024, capturing the hydrological dynamics leading up to, during, and after the flood event. During this period, the average discharge was 1,713 m³/s, with the minimum flow recorded at 461 m³/s on February 19 and the maximum at 3,068 m³/s on March 4. On the day of the peak event—March 6—the river flow was 2,549 m³/s, which, although not the highest during the period, coincided with a rapid rise in water level.

Water levels exceeded critical thresholds, with values surpassing the official overflow level of 14 meters. On March 6, the river reached 17.87 meters, approaching the historical maximum of 18.30 meters recorded during the 2015 flood. The alert level for the river is set at 13.5 meters, with 14 meters marking the overflow threshold. Thus, the 2024 event represents an extreme hydrological episode, as water levels rose well above both limits. Even though the corresponding discharge was not the highest observed during the event window, the magnitude of the water level confirms the severity of the flood.

This event is considered the second most significant flood ever recorded in this section of the Acre River, both in terms of river stage and socioeconomic impact. The decoupling between peak discharge and peak water level also underscores the complex interaction between channel morphology, backwater effects, and catchment response, emphasizing the importance of high-resolution hydraulic modeling in flood risk assessments.

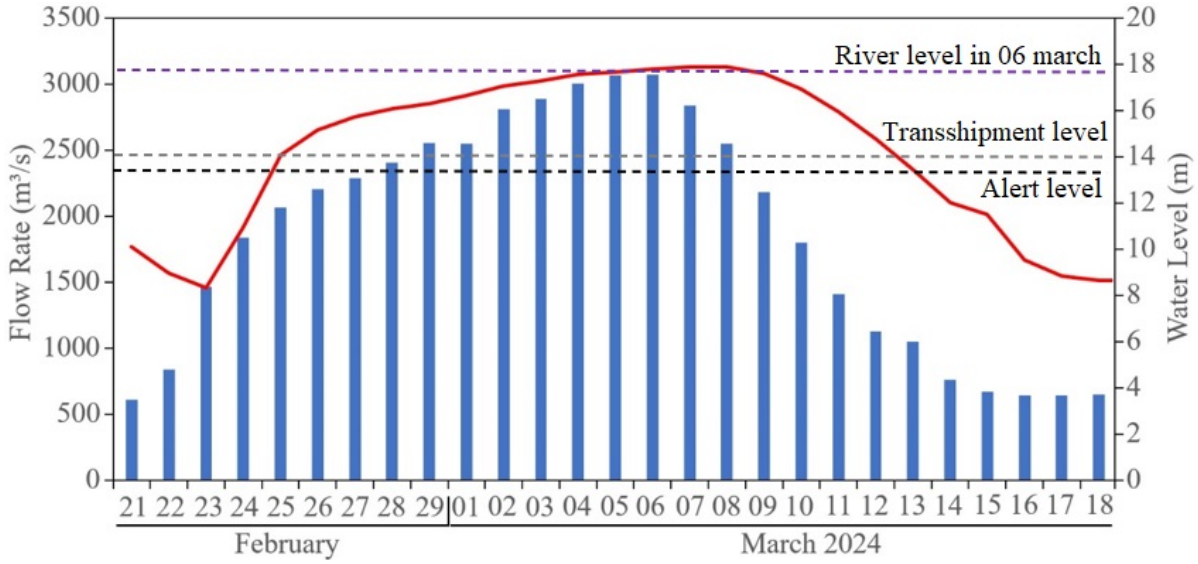

Fig 6. Daily variability of river flow rate (m³/s) and water level (m) between February 21 and March 18, 2024, highlighting the dynamics leading up to and during the peak flood event on March 6.

Impacts of the Floods in Rio Branco, Acre, in March 2024

Flood map

Table 9 provides a comprehensive summary of the flood impacts observed during the peak event on **March 6, 2024**, and the post-peak conditions on **March 18, 2024**. The data include flooded area (in hectares), rainfall accumulation, river discharge, water level, and spatial impact metrics such as affected census sectors, urban areas, and building footprints. These indicators are critical for evaluating the severity and spatial extent of the flood and for identifying priority areas for emergency response and long-term resilience planning.

The inclusion of both hydrometeorological variables (rainfall, flow rate, river level) and socio-spatial parameters (census sectors, urban zones, and built-up areas) offers a multidimensional perspective on the flood's impact. It also captures the dynamic nature of the event, including the rapid expansion and subsequent recession of floodwaters. Additionally, records of municipalities in a state of emergency and sites with confirmed fatalities allow for a more granular understanding of the disaster's implications for both infrastructure and population vulnerability.

Table 9. Summary of flood impacts during the March 6–18, 2024 period, including total flooded area (ha), cumulative rainfall (mm), flow rate (m^3/s), river level (m), and extent of affected areas by census sector, urban footprint, and buildings (ha), comparing conditions at flood peak (March 6) and post-peak (March 18).

Classes	Peak Flow (4 6 2024)	Post-Peak (4 18 2024)
Flood (ha)	3197.19	1693.51
Rainfall/Prelim/Pentad (mm)	52.17	0.00
Flow Rate (m^3)	2835	725.2
River Level (m)	17.87	10.44
Census sectors (ha)	3257.25	1725.34
Urban areas (ha)	1459.85	823.53
Buildings (ha)	158.84	72.31

Figure 7 presents the simulated flood extent for the municipality of **Rio Branco**, corresponding to the peak event on **March 6, 2024**. The map highlights the **maximum water level of 17.7 meters**, recorded at the ANA monitoring station, and visualizes the spatial distribution of inundated areas across the city. Districts affected by the flood are shaded in gray, while flooded buildings are indicated in black. The depth gradient, ranging from 0 to 17.7 meters, is represented by a blue scale, illustrating the variation in flood intensity across the landscape.

Subfigure **(a)** shows a high-resolution satellite image with the overlay of the maximum flood extent, confirming inundation along the Acre River and its tributaries, especially in densely built-up areas. Subfigure **(b)** displays the spatial distribution of **Curve Number (CN)** values, which influence surface runoff potential. Areas with high CN values—corresponding to low infiltration capacity—are mostly located in urbanized zones, reinforcing their susceptibility to flooding. Subfigure **(c)** illustrates the **infiltration capacity** of the soil, with lower infiltration rates aligned with the flooded regions, particularly along the urban fringe and floodplain zones.

The bar chart at the bottom quantifies the area affected by flooding in each district, with some sectors such as ***Seis de Agosto***, ***Base***, **and** ***Preventório*** exceeding 200 hectares of inundation. The spatial correlation between topography, land use, and hydrological response is evident, supporting the results of the hydraulic model.

According to field reports from the **Geological Survey of Brazil (SGB)** and **Civil Defense**, the observed water level of the Acre River during the flood event reached **1.89 meters above the overflow threshold**, reinforcing the classification of the March 2024 event as one of the most severe floods in recent decades.

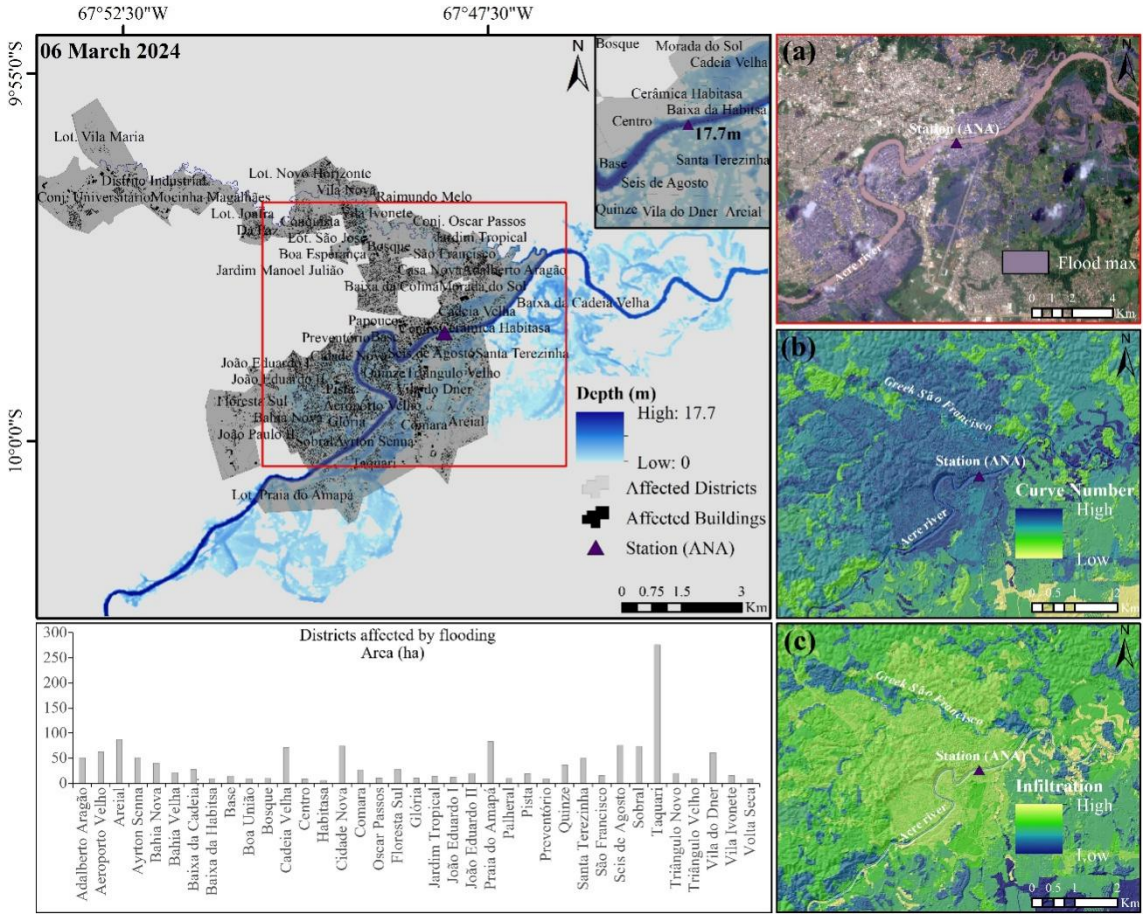

Fig 7. Flood map of Rio Branco and affected neighborhoods during the event on March 6, 2024, indicating the maximum river level (17.7 m) recorded at the fluviometric station. (a) Simulated flood

extent overlaid on a false-color composite from the Sentinel-2 MSI sensor; (b) Curve Number (CN) map representing runoff potential; (c) Infiltration capacity map derived from soil and land cover data.

Figure 8 provides a comparative analysis of the Acre River and its surrounding landscape using false-color composite images derived from the Sentinel-2 MSI sensor, acquired before (February 15, 2024) and after (March 11, 2024) the flood event. These images allow for a clear visualization of changes in water extent and land surface conditions associated with the March 2024 flood. The pre-event image (Figure 8a) shows the river in its regular channel width under normal hydrological conditions, while the post-event image (Fig. 8b) reveals a substantial increase in surface water extent, particularly along the floodplain and urban areas. Insets (Fig. 8a and 8b) emphasize the marked expansion of the river channel during the peak flood period, demonstrating the spatial magnitude of inundation and supporting the simulation results presented earlier. This satellite-based visual comparison reinforces the observed severity of the event and provides geospatial evidence for validating the hydrodynamic model outputs.

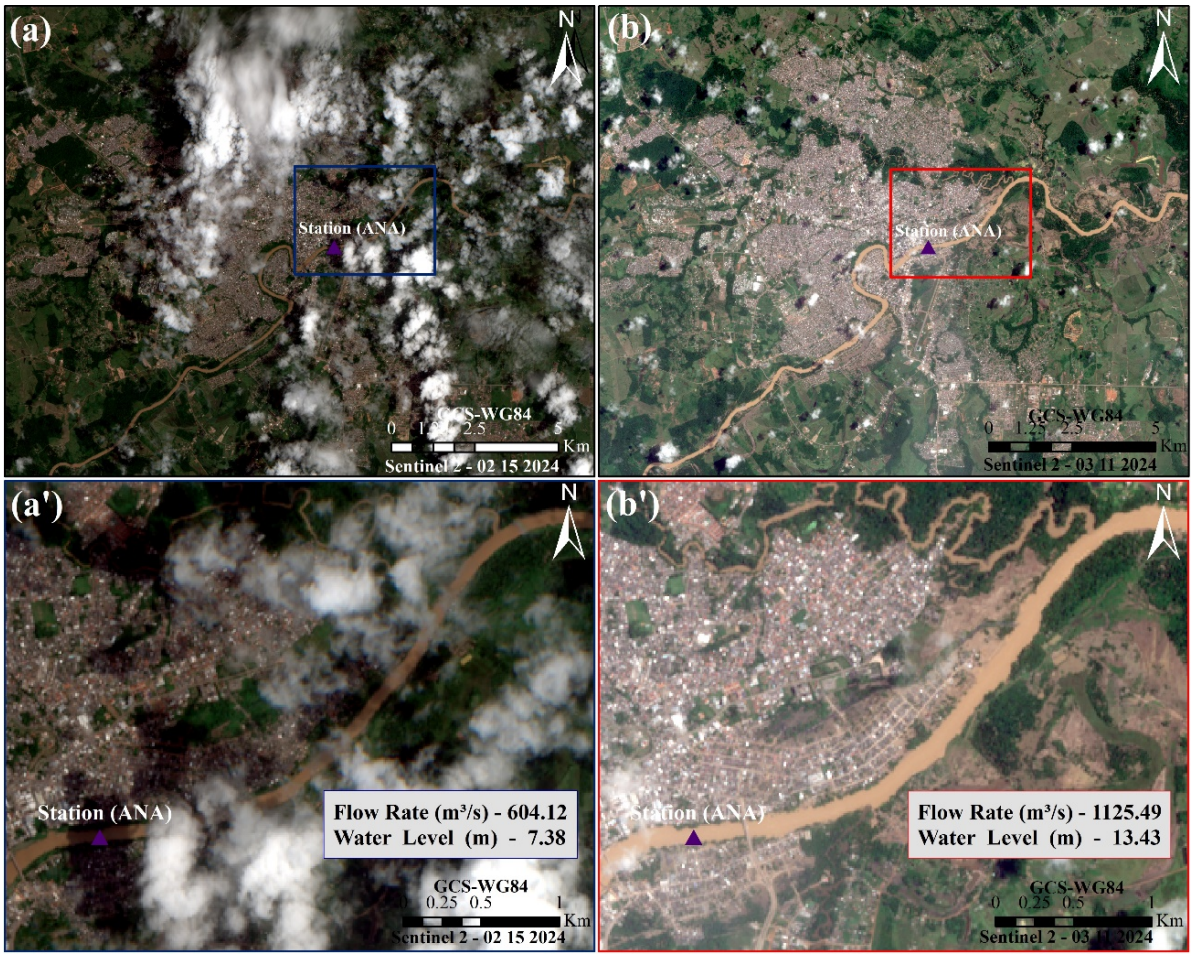

Fig. 8 (a) False-color image from the MSI sensor onboard Sentinel-2 acquired before the flood event (February 15, 2024); (b) False-color image acquired after the event (March 11, 2024). Insets (a′; b′) highlight the expansion of the Acre River channel and inundated areas following the flood.

Figure 9 presents the comparison between observed and simulated water level time series at the ANA fluviometric station, covering the period surrounding the March 2024 flood event. The two series exhibit strong agreement in both magnitude and temporal behavior, with errors around 10%, indicating that the hydrodynamic model was able to accurately replicate the river's physical response. This close alignment supports the reliability of the simulation and confirms that the model calibration adequately reflects the hydrological conditions of the Acre River.

Model performance was quantitatively evaluated using the **Nash–Sutcliffe Efficiency (NSE)**, which yielded a value of **0.99**. This metric is widely applied in hydrological modeling to assess how well simulated data approximate observed measurements. An NSE value close to 1.0 suggests excellent model performance, with the simulation reproducing nearly all observed variability. In this case, the value of 0.99 indicates that the model explains approximately 99% of the variance in the observed data, a result that confirms the robustness of the calibration and the credibility of the simulated flood dynamics. Such high accuracy ensures that the model outputs are suitable for subsequent flood risk and hazard assessments.

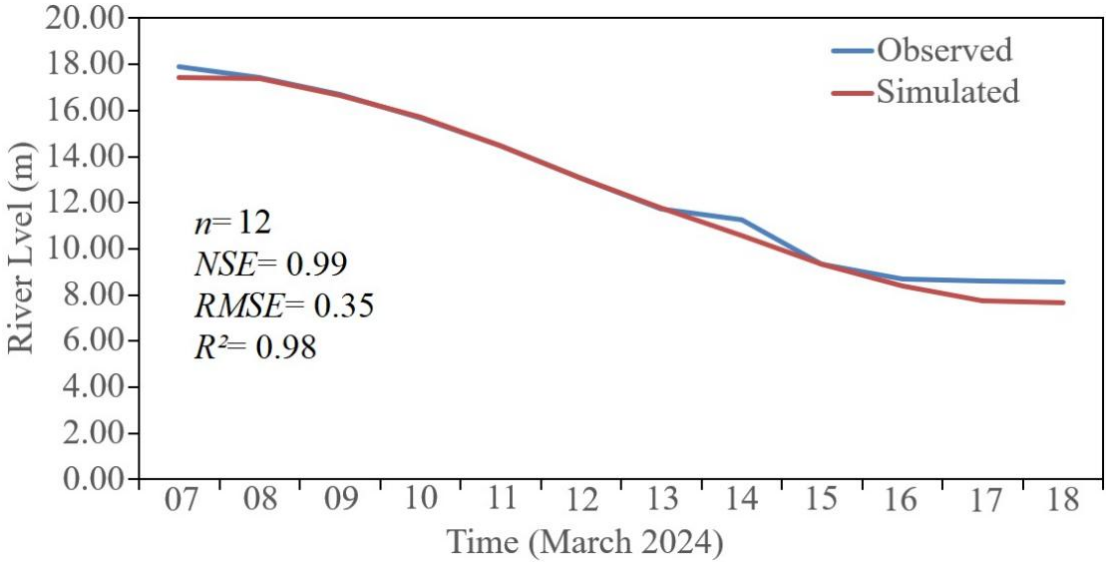

Fig 9. Validation of the flood model using observed versus simulated river levels at the ANA station. The close agreement between the time series supports the model's accuracy and reliability.

The Standard Deviation Ratio (RSR) obtained for the model validation was **0.01**, which indicates an excellent agreement between observed and simulated river levels. The RSR is a widely used goodness-of-fit metric in hydrological modeling, calculated as the ratio between the root mean square error (RMSE) of the model residuals and the standard deviation of the observed data. An RSR value approaching zero reflects minimal residual error and high model accuracy.

In this case, an RSR of 0.01 implies that the standard deviation of the model residuals is only about **1% of the variability** present in the observed dataset, signifying that the model not only reproduces the central tendency of the river levels but also effectively captures their variability and dynamic behavior. Values below 0.5 are generally interpreted as indicative of good model performance, and values close to zero, as seen here, denote **very high predictive precision**. When interpreted alongside the NSE score of 0.99, this RSR value reinforces the robustness and reliability of the calibrated hydrodynamic model in simulating flood conditions for the Acre River.

Figure 10 illustrates the spatial distribution of **flood risk** (panel a) and **hazard rating** or **risk to people** (panel b) for the urban area of Rio Branco, based on hydrodynamic modeling and geospatial vulnerability assessment. The maps classify areas according to severity levels ranging from *low* to *extreme*, providing critical insights into zones most susceptible to flooding and those where human exposure to danger is highest. The classifications integrate flood depth, land use, population density, and infrastructure distribution, aligning with FEMA and DEFRA methodologies for flood risk and hazard assessment.

Panel **(a)** shows the flood risk classification, with extensive areas—particularly along the Acre River and its floodplain—classified as **high**, **very high**, or **extreme** risk. These areas include dense urban neighborhoods such as *Seis de Agosto*, *Centro*, *Ayrton Senna*, and *Taquari*. Panel **(a)** zooms into a critical segment of the city and identifies key affected districts, marked with green circles, highlighting zones where flood exposure is most pronounced.

Panel **(b)** presents the hazard rating, which reflects not only flood depth but also potential harm to individuals based on exposure and vulnerability indicators. The hazard map reveals that large portions of the central and southern districts face **significant to extreme hazard levels**, indicating elevated risks to life and infrastructure. Panel **(b′)** further details these conditions within the same subregion highlighted in (a′), confirming that neighborhoods previously identified with extreme flood risk also correspond to areas of high hazard to people.

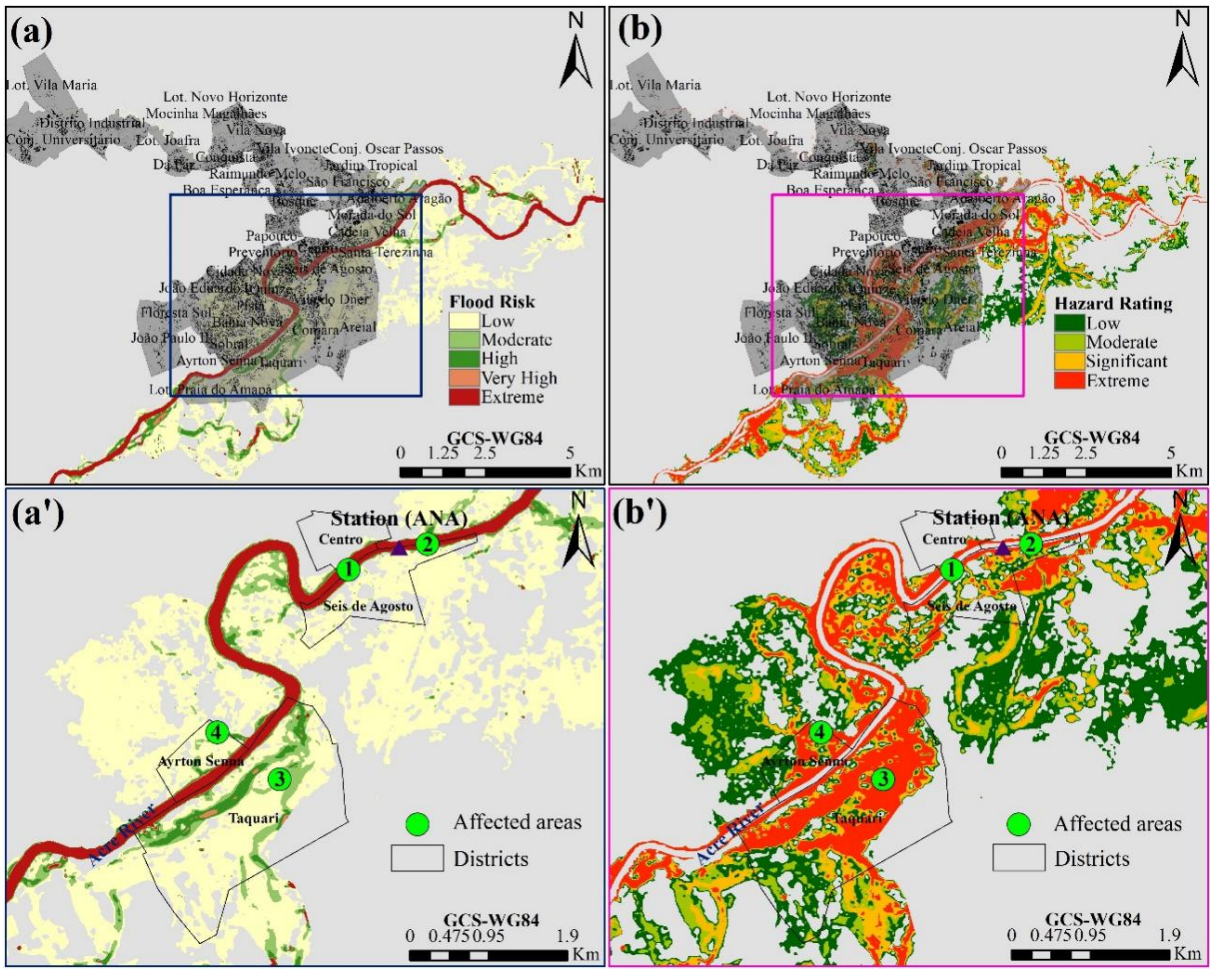

Fig 10. (a) Flood risk classification and (b) hazard rating (risk to people) for the city of Rio Branco, showing spatial variation from low to extreme levels. Insets (a′) and (b′) highlight key districts affected by flooding and areas where population exposure to flood-related hazards is highest.

Figure 11 presents photographic evidence of the flood impacts in key locations across Rio Branco during the March 2024 event. These images offer a visual complement to the model-based analyses, confirming the extent and severity of inundation in both central and peripheral urban areas. Panel **(1)** shows the historic city center near the ANA fluviometric station, including major infrastructure elements such as the Juscelino Kubitschek metal bridge, the Joaquim Macedo pedestrian walkway, and the Colonel Sebastião Dantas bridge—all partially submerged or surrounded by floodwaters. Panel **(2)**, also taken near the monitoring station, highlights the flooding around the newly constructed Fourth Bridge, underscoring the widespread nature of the inundation even in recently developed areas.

Panel **(3)** captures the situation in the **Taquari** neighborhood, a densely populated district with low-lying topography that has been recurrently affected by flood events. Panel **(4)** shows the **Ayrton Senna** neighborhood, another high-risk area identified in the hazard classification maps, further illustrating the alignment between modeled results and real-world impacts. These photographs serve as critical validation of the hydrodynamic model outputs

and provide tangible evidence of the socioeconomic exposure across different zones of the city.

Fig. 11 Photographs of flooded locations in Rio Branco during the March 2024 event. (1) City center near the fluviometric station, showing the Juscelino Kubitschek metal bridge, Joaquim Macedo walkway, and Colonel Sebastião Dantas bridge; (2) Fourth Bridge area, also near the station; (3) Taquari neighborhood; (4) Ayrton Senna neighborhood.

Tables 10 and 11 summarize the spatial extent of flood risk and hazard classifications across Rio Branco for the peak flood date of **March 6, 2024**, providing quantitative support for the visual analyses presented earlier. **Table 10** presents the total area affected in hectares and as a percentage, disaggregated by flood risk level (low to extreme) and hazard rating (low to extreme). The results show that **extreme flood risk** affected approximately **373.03 hectares (11.69%)**, while the **extreme hazard class**, representing the highest level of risk to people, accounted for **787.20 hectares (27.52%)** of the total area assessed. Most of the study area falls into the **low risk (73.11%)** and **low hazard (36.60%)** categories, yet the significant presence of moderate to extreme classes highlights critical zones of vulnerability.

Table 10. Area (in hectares and percentage) classified by flood risk and hazard rating levels for March 6, 2024, in the urban area of Rio Branco.

Flood Risk	Area (ha)	Area (%)	Hazard Rating	Area (ha)	Area (%)
Low	2334.78	73.11	Low	1046.65	36.60
Moderate	248.56	7.78	Moderate	452.55	15.82
High	187.16	5.86	Significant	573.19	20.06
Very High	49.92	1.56	Extreme	787.2	27.52
Extreme	373.03	11.69	---	---	---
Total	3193.45	100	Total	2859.59	100

Table 11 complements these findings by detailing the total area of **census sectors, urban zones, and buildings** affected by both flood risk and hazard rating classifications. The data reveal that approximately **3,195 hectares of census sectors** were impacted under flood risk assessment, and **2,913 hectares** under hazard rating. Urban areas affected totaled **1,401 hectares** and **1,339 hectares**, respectively. In terms of the built environment, **buildings affected** reached **147.24 hectares under flood risk** and **151.98 hectares under hazard rating**, reinforcing the significant exposure of critical infrastructure and residential areas. These metrics underscore the importance of spatially targeted risk mitigation strategies, particularly in densely populated and infrastructurally vital sectors.

Table 11. Area in hectares of the census sector, Urban area and Buildings affected by the flood in hectares, the Urban area affected by Flood Risk and Hazard Rating for the day 06 march, 2024.

Classes	Flood Risk	Hazard Rating
Census Sectors (ha)	3194.84	2913.33
Urban Areas (ha)	1401.27	1339.53
Buildings (ha)	147.24	151.98

Figure 12 presents a categorical breakdown of flood risk distribution across different land use and land cover (LULC) classes and census sector typologies in the city of Rio Branco. Panel **(a)** classifies flooded areas according to LULC types, revealing that the largest portions of land affected fall within **pasture**, **urban infrastructure**, and **built-up areas** (including buildings and districts). These land cover types show considerable exposure to **high**, **very high**, and **extreme flood risk** levels, indicating the vulnerability of both rural agricultural zones and densely urbanized sectors.

Panel **(b)** organizes flood risk levels by census sector classifications, showing that **high-density urban areas** represent the most significantly affected category. Notably, this

sector includes substantial portions of land under both **moderate** and **extreme flood risk**, reinforcing the importance of prioritizing densely populated regions in flood mitigation strategies. Low-density and rural areas are also affected, but to a lesser extent and with greater spatial heterogeneity in risk levels. Together, these charts underscore the spatial variability of flood risk and the need to tailor adaptation measures based on both land use and population distribution characteristics.

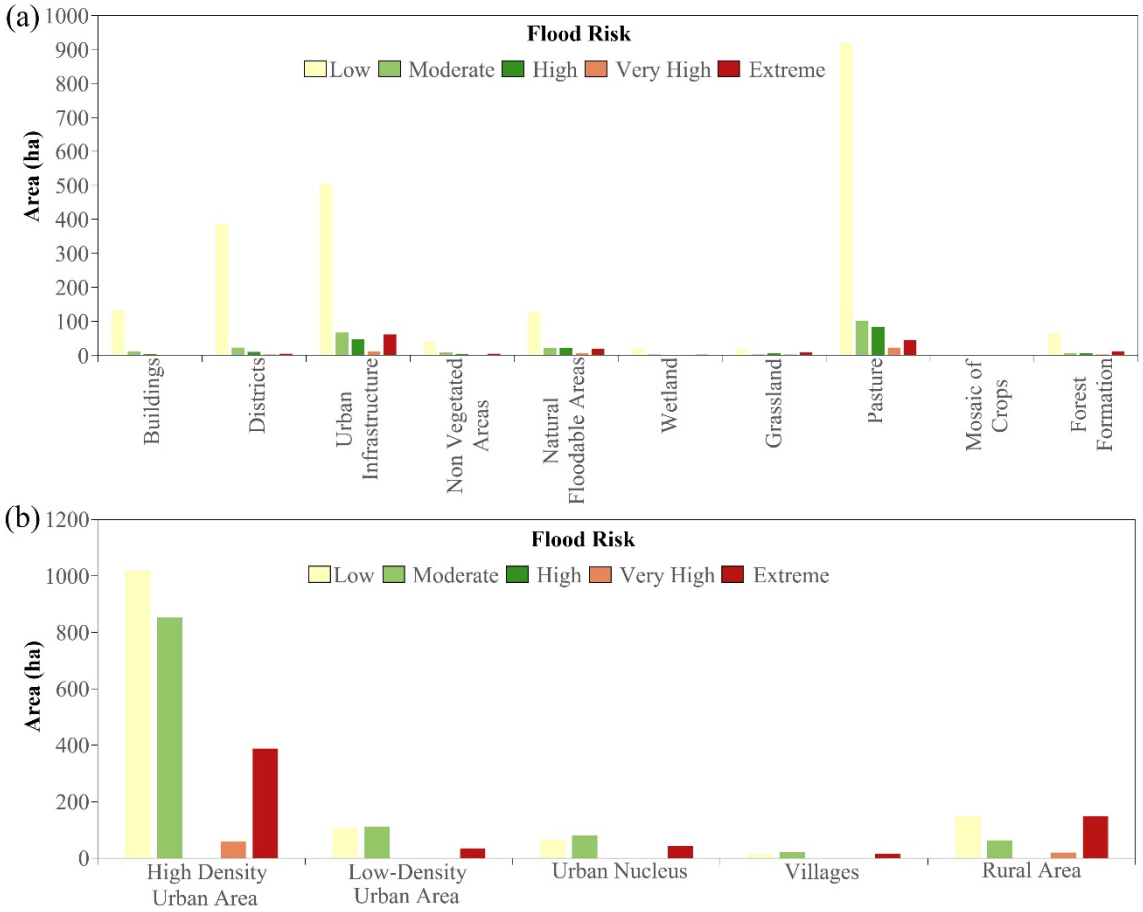

Fig 12. (a) Area (ha) per flood risk class by land use and land cover (LULC) category; (b) Area (ha) per flood risk class by census sector typology, for March 6, 2024.

Figure 13 presents the classification of **hazard rating areas** for the March 6, 2024 flood event, based on land use and land cover (LULC) classes and census sector typologies. These hazard ratings account not only for flood depth and extent, but also for potential human exposure and vulnerability within each spatial category.

Panel **(a)** categorizes affected areas by LULC classes and shows that the most significant hazard levels are concentrated in **pasture lands**, **urban infrastructure**, and **built-up areas** (e.g., buildings and districts). Notably, urban infrastructure exhibits a substantial portion of land under the **extreme hazard class**, highlighting the increased risk to human populations and critical assets in highly urbanized zones. Pasture areas also display elevated hazard ratings, which may be associated with rapid runoff and lack of protective infrastructure.

Panel **(b)** shows the distribution of hazard levels across different census sector types. **High-density urban areas** dominate the affected territory, with considerable land area falling under **significant** and **extreme hazard** ratings. **Low-density urban zones** and **rural areas** are also exposed to various hazard levels, though with more spatial heterogeneity. These results reinforce the critical need for differentiated risk management strategies that consider both land use patterns and population concentration.

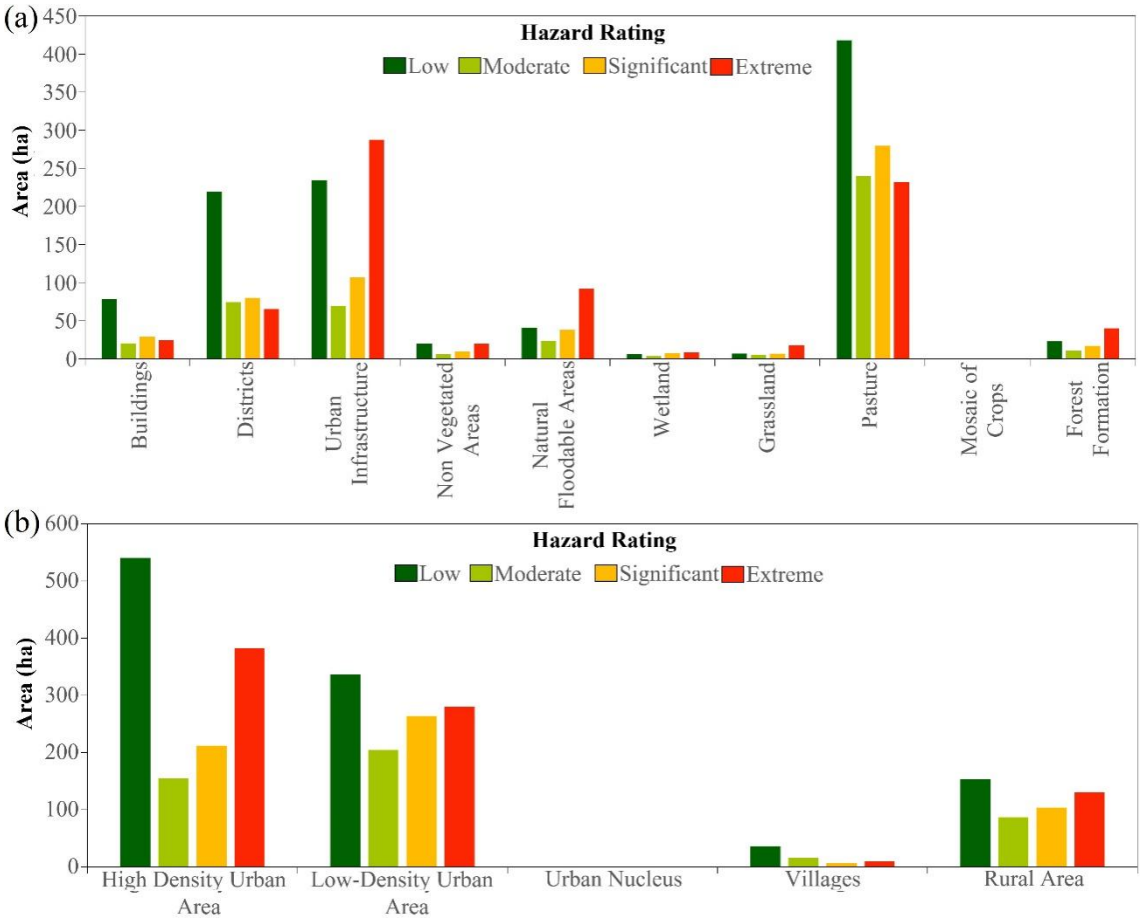

Fig 13. (a) Area (ha) per hazard rating class by land use and land cover (LULC) category; (b) Area (ha) per hazard rating class by census sector typology, for March 6, 2024

Figure 14 presents the distribution of flood impact across the various **districts** of Rio Branco on **March 6, 2024**, based on both flood risk classification and hazard rating. Panel **(a)** illustrates the total area (in hectares) affected per district, categorized by flood risk levels (from low to extreme). The results highlight that several densely populated districts—such as **Seis de Agosto**, **Taquari**, and **Centro**—experienced significant exposure to **very high** and **extreme flood risk**, reflecting their location along the floodplain and proximity to the Acre River.

Panel **(b)** complements this analysis by showing the area affected per hazard rating class in each district, considering potential risk to people. Districts such as **Triângulo Novo**, **Seis de Agosto**, **Santa Terezinha**, and **Centro** show large areas under **extreme hazard**,

indicating zones with high vulnerability due to both exposure and population density. Meanwhile, some peripheral districts display larger areas under **low to moderate hazard**, reflecting reduced human exposure or greater infiltration capacity in those zones.

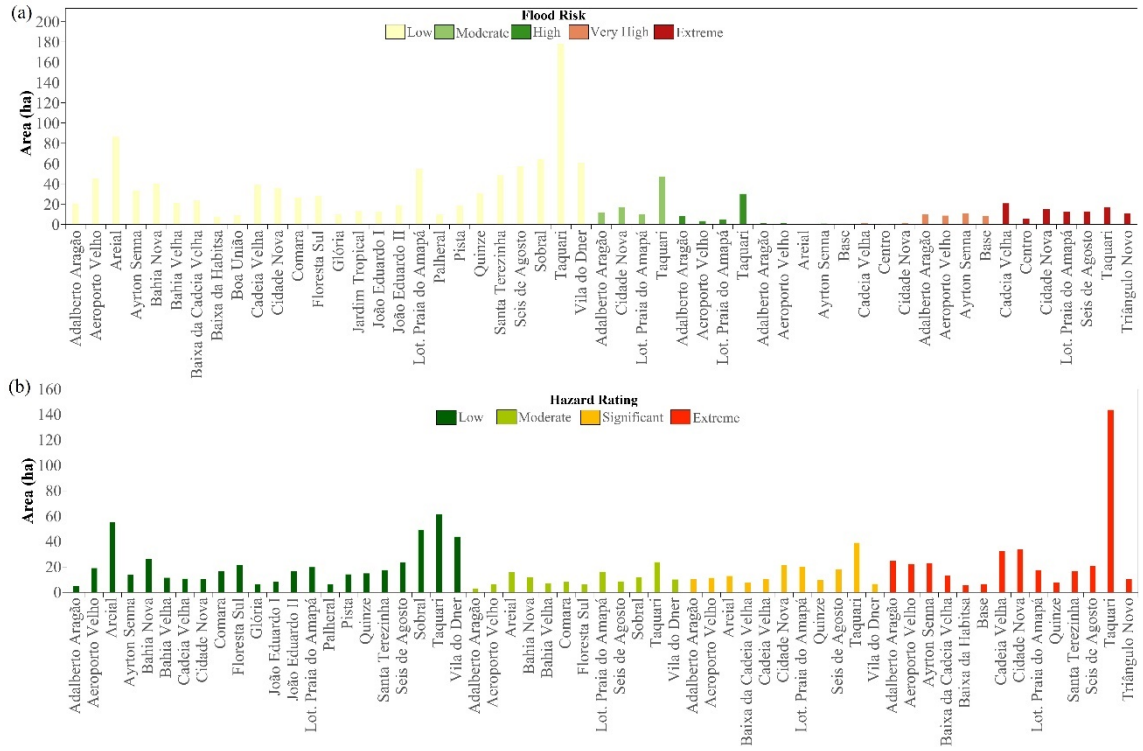

Fig 14. (a) Area (ha) per flood risk class by district; (b) Area (ha) per hazard rating class by district, for March 6, 2024

Discussion

Urban Flood Exposure and Socio-environmental Vulnerability

The spatial distribution of flood-prone areas in Rio Branco, particularly in low-lying urban districts such as Seis de Agosto and Cadeia Velha, reflects long-standing patterns of unregulated expansion into floodplains. The 2024 flood event confirmed the high exposure of socially vulnerable populations to recurrent hydrological hazards. Similar spatial dynamics were identified in Cruzeiro do Sul during the 2021 flood, where flood impacts were concentrated in urban neighborhoods located along the Juruá River (Mantovani et al. 2024). These findings reinforce the critical importance of risk-sensitive territorial planning that incorporates both physical hazard modeling and socio-environmental vulnerability indicators.

Hydrological Extremes and La Niña Influence

The 2024 flood occurred during a La Niña year and exhibited characteristics consistent with other extreme events driven by strengthened Walker circulation. The increase in atmospheric upward motion over northern Amazonia during La Niña phases has been linked to enhanced deep convection and increased rainfall (Barichivich et al. 2018). Espinoza et al. (2022) observed that, since the late 1990s, extreme floods in the Amazon Basin have become

more frequent, with several events surpassing historic thresholds. In Acre, Silva et al. (2023) documented 202 extreme events between 1987 and 2023, with a marked increase after 2010. The city of Rio Branco alone recorded 14 state-declared emergencies, mostly related to flooding. These regional trends point toward a hydrological regime increasingly influenced by large-scale climate variability and its compounding effects on flood severity.

Trends in Rainfall and Streamflow

Although long-term rainfall and discharge records in Rio Branco do not show statistically significant monotonic trends, several studies have identified linear upward tendencies in both variables. Oliveira et al. (2021) detected a gradual increase in maximum daily rainfall and river discharge, suggesting changes in the intensity rather than frequency of extremes. While the Mann-Kendall and Spearman tests did not confirm statistical significance at the 5% level, the recurrence of flood disasters and increases in design quantiles point to a shift in hydrological behavior that aligns with broader observations in the Amazon. These results also highlight the limitations of relying exclusively on trend detection tests to assess flood risk in rapidly changing climatic contexts.

Floodplain Processes and Sediment Feedbacks

Floodplain dynamics in Amazonia are regulated by complex interactions between hydrology, sediment transport, and ecological feedbacks. According to Feng et al. (2025), sediment deposition in the floodplains of the Amazon and Solimões rivers is governed more by hydrodynamic conditions than by water level alone. This reinforces the importance of considering sediment redistribution in long-term flood hazard assessments. In addition, Van der Sleen et al. (2025) demonstrate that extreme flood events combined with wildfire occurrence—particularly in floodplains of black-water rivers—can compromise ecosystem resilience and delay post-disturbance recovery. Although the Acre River is characterized as a white-water system with higher nutrient loads, similar interactions between flood pulses and land cover degradation may be contributing to the intensification of flood impacts in the region.

Advances in Modeling and Risk Mapping

The present study employed HEC-RAS 2D modeling with unsteady flow to simulate flood extents under the 2024 event, integrating high-resolution topography, land use, and soil data. This approach is consistent with Mantovani et al. (2024), who applied similar methods in Cruzeiro do Sul and found strong agreement between model predictions and observed flood extents. The use of validated hazard rating methodologies from DEFRA (2006) and risk

frameworks from FEMA (2018) further supports the robustness of the risk maps produced. The accuracy of the 2024 flood simulation reinforces the value of coupling hydrodynamic models with socio-spatial data for producing actionable flood risk maps. These tools are essential for guiding disaster preparedness, emergency response, and long-term adaptation strategies in flood-prone urban regions of the Amazon.

Conclusion

The flood event of March 2024 in Rio Branco, Acre, stands as a critical manifestation of escalating hydroclimatic extremes in the southwestern Amazon. Although long-term trends in rainfall and streamflow did not reach statistical significance, the recurrence and severity of recent flood events—especially those coinciding with La Niña phases—demonstrate an intensification of hydrological extremes not adequately captured by trend analysis alone.

The flood modeling presented in this study, based on 2D hydrodynamic simulation and refined topographic inputs, closely reproduced the spatial dynamics observed during the event. The resulting risk and hazard maps revealed that a substantial portion of the urban territory, including high-density neighborhoods, is consistently exposed to life-threatening flood conditions. These areas coincide with zones of social vulnerability, underscoring a pattern of risk accumulation driven by unplanned urban growth along river margins.

The findings point to a structural mismatch between the scale of the hydrometeorological threat and the current capacity of urban planning and disaster risk governance to address it. In this context, the conclusion is clear: **the intensification of flood events in Rio Branco is not an anomaly—it is a trajectory**.

Adaptation must therefore move beyond emergency response toward anticipatory strategies grounded in spatial planning, early warning, and integrated risk governance. This study contributes to that shift by providing technically validated evidence of flood dynamics and spatial risk patterns under current climatic conditions. The implication is urgent: **cities in the Amazon region must revise their assumptions about flood recurrence and proactively integrate risk-informed planning into public policy**.

References

Alcântara E, Marengo J, Mantovani J, Londe LR, San LY, Park E, Lin YN, Wang J, Mendes T, CunhaAP, Pampuch L, Seluchi ME, Simões S, Cuartas LA, Goncalves D, Massi K, Alvalá RCS, MoraesOL, Souza Filho C, Mendes R, Nobre CA (2023) Deadly disasters in southeastern South America:flash floods and landslides of February 2022 in Petrópolis, Rio de Janeiro. Nat Hazards Earth Syst Sci23:1–19. https://doi.org/10.5194/nhess-23-1-2023.

Alcântara E, Baião CF, Guimarães YC, Marengo JA, & Mantovani JR (2024) Climate change-induced shifts in landslide susceptibility in São Sebastião (Southeastern Brazil). Natural Hazards Research. Available online 28 November 2024, In Press.

Al-Zahrani J (2017) Estimation of Natural Radioactivity in Local and Imported Polished Granite Used as Building Materials in SaudiArabia. J. Radiat. Res. Appl. Sci. 2017, 10, 241–245. [CrossRef]

Barichivich J, Gloor M, Peylin P, Brienen RJW, Schöngart J, Espinoza JC, & Phillips OL (2018) Recent intensification of Amazon flooding extremes driven by strengthened Walker circulation. *Science Advances*, 4(8), eaat8785

Beden N, & Keskin AU (2021) Flood map production and evaluation of flood risks in972 situations of insufficient flow data. Natural Hazards 105, 2381– 2408 (2021). Available973 at: https://doi.org/10.1007/s11069-020-04404-y

Costabile P, Costanzo C, De Lorenzo G, De Santis R, Penna N, Macchione F (2021) Terrestrial and airborne laser scanning and 2-D modelling for 3-D flood hazard maps in urban areas: new opportunities and perspectives Environ. *Environ. Model. Softw.* 2021, *135*, 104889

Davis CV, Sorensen KE (1969) Handbook of Applied hydraulics. 3. ed. Chicago: McGraw-Hill Book Company, 1969

Department for Environment, Food & Rural Affairs-DEFRA (2006) *Flood Risk Assessment Guidance for New Development: FD2320/TR2*. London: Environment Agency

Dunn RJH, Herold N, Alexander LV, Donat MG, Allan R, Bador M, et al (2024) Observed global changes in sector-relevant climate extremes indices - an extension to hadEX3. Earth and Space Science 11, (2024). Available at: https://doi.org/10.1029/2023EA003279

Espinoza JC, Marengo JA, Schöngart J, & Jimenez JC (2022). The new historical flood of 2021 in the Amazon River compared to major floods of the 21st century: Atmospheric features in the context of the intensification of floods. *Weather and Climate Extremes*, 35, 100406

Federal Emergency Management Agency (FEMA) (2018) Guidance for flood risk analysis and mapping, USA, (2018)

Feng D, Syvitski JPM, Park E, & Lavel L, (2025) Floodplain sedimentation in the Amazon: Hydrodynamic controls and implications for hazard modeling. *Nature Communications*, 16, 57495

Funk C, Peterson P, Landsfeld M, Pedreros D, Verdin J, Shukla S, Michaelsen J (2015) The climate hazards infrared precipitation with stations—A new environmental record for monitoring extremes. *Sci. Data* 2015, *2*, 150066. https://doi.org/10.1038/sdata.2015.66.

Haidu I, Batelaan O, Crăciun AI, Domniţa M (2017) GIS module for the estimation of the hillslope torrential peak flow. Environ Eng Manag J 16(5):1137–1144 *(PDF) Romanian River Basins Lag Time Analysis. The SCS-CN Versus RNS Comparative Approach Developed for Small Watersheds*

Hosseini T, Fathivand A, Barati, H, Karimi M (2006) Assessment of radionuclides in imported

foodstuffs in Iran. J. Radiat. Res. 2006,4, 149–153

Hyndman RJ, Koehler AB (2006) Another look at measures of forecast accuracy. *Int. J. Forecast.* 2006, *22*, 679–688. https://doi.org/10.1016/j.ijforecast.2006.03.001

IBGE. Instituto Brasileiro de Geografia e Estatística. Available online: https://www.ibge.gov.br/en/geosciences/territorial-organization/territorial-organization/28114-malhas-de-setores-censitarios-divisoes-intramunicipais-2.html?lang=en-GB (accessed on 24 January 2025)

IPCC. Climate Change 2022: Impacts, Adaptation and Vulnerability. Contribution of Working Group II to the Sixth Assessment Report of the Intergovernmental Panel on Climate Change; Cambridge University Press; Cambridge University Press: Cambridge, UK; New York, NY, USA, 2022; p. 3056. https://doi.org/10.1017/ 9781009325844, 2022

IPCC. Climate Change, 2023. Synthesis Report. A Report of the Intergovernmental Panel on Climate Change. Contribution of Working Groups I, II and III to the Sixth Assessment Report of the Intergovernmental Panel on Climate Change; Core Writing Team, Lee, H., Romero, J., Eds.; IPCC: Geneva, Switzerland, 2023

Kim D, Lee JY, Yang JS, Kim JW, Kim VN, Chang H (2020) The Architecture of SARS-CoV-2 Transcriptome. *Cell* 2020, *181*, 914–921.e10. https://doi.org/10.1016/j.cell.2020.04.011

Mantovani J, Alcântara E, Marengo JA, Londe L, Park E, Cunha AP, Tomasella J (2024) Flood Risk Mapping during the Extreme February 2021 Flood in the Juruá River, Western Brazilian Amazonia, State of Acre. Sustainability 2024, 16, 2999. https://doi.org/10.3390/su16072999

Mantovani J, Alcântara E, Pampuch LA *et al* (2024) Assessing flood risks in the Taquari-Antas Basin (Southeast Brazil) during the September 2023 extreme rainfall surge. *npj Nat. Hazards* 1, 9 (2024). https://doi.org/10.1038/s44304-024-00009-8

Mantovani JR, Alcântara E, Baião CF, Pampuch L, Curtarelli MP, Mariano Ribeiro JV, Guimarães YC, Londe L, Massi K, Marengo J, Nobre CA, Assireu AT, Bortolozo CA, Simões SJ, Tomasella J, Leal de Moraes OL, Park E (2024) Unprecedented Flooding in Porto Alegre Metropolitan Region (Southern Brazil) in May 2024: Causes, Risks, and Impacts, *Journal of South American Earth Sciences*, https://doi.org/10.1016/j.jsames.2025.105533

Marengo J, Alcântara E, Cunha A, Seluchi M, Nobre C, Dolif G, Goncalves D, Assis Dias M, Cuartas L, Bender F, Ramos A, Mantovani J, Alvalá R, & Moraes O (2023) Flash floods and landslides in the city of Recife, northeast Brazil after heavy rain on May 25–28, 2022: Causes, impacts, and disaster preparedness. Weather and Climate Extremes 39, 1-17 (2023)

Marengo JA, Cunha AP, Seluchi ME *et al* (2024) Heavy rains and hydrogeological disasters on February 18th–19th, 2023, in the city of São Sebastião, São Paulo, Brazil: from meteorological causes to early warnings. *Nat Hazards* (2024). https://doi.org/10.1007/s11069-024-06558-5

McCuen RH, Knight Z, Cutter AG (2006) Evaluation of the Nash–Sutcliffe efficiency index. J. Hydrol. Eng. 2006, 11, 597–602. [CrossRef]

Moriasi DN, Arnold JG, Van Liew MW, Bingner RL, Harmel RD, Veith TL (2007) Model Evaluation Guidelines for SystematicQuantification of Accuracy in Watershed Simulations. (PDF). Trans. ASABE 2007, 50, 885–900. [CrossRef]

Muthusamy M & Rivas-Casado M, & Butler, D, & Leinster, P (2021) Understanding the effects of Digital Elevation Model resolution in urban fluvial flood modelling. Journal of Hydrology. 596. 126088. 10.1016/j.jhydrol.2021.126088

Nash JE, Sutcliffe JV (1970) River Flow Forecasting through Conceptual Model. Part 1—A Discussion of Principles. *J. Hydrol.* 1970, *10*, 282–290. https://doi.org/10.1016/0022-1694(70)90255-6

NATURAL RESOURCES CONSERVATION SERVICE – NRCS (2009) Chapter 7: Hydrologic soil groups. In: National engineer-ing handbook: Part 630, Hydrology. Available: http://directives.sc.egov.usda.gov/

Nimer E (1977) Clima. In Geografia do Brasil: Região Norte; IBGE: Rio de Janeiro, Brazil, 1977; Volume 1, pp. 39–58

Oliveira AV, Serrano ROP, Mesquita AA, & Moreira JGV (2021) Temporal trend and estimation of the hydrological risk of maximum rainfall and flow extremes in the city of Rio Branco, Acre, Brazil. *Revista Brasileira de Meteorologia*, 36(4), 749–758

Ponce V.M, Lugo A (2001) Modeling looped ratings in Muskingum-Cunge routing. J. Hydrol. Eng. ASCE 2001, 6, 119–124. [CrossRef]

Rafiei-Sardooi E, Azareh A, Choubin B, Mosavi AH, and Clague JJ (2021) Evaluating urban flood risk using hybrid method of TOPSIS and machine learning. Int. J. Disaster Risk Reduc. 66, 102614. https:// doi.org/10.1371/journal.pone.0233570

Ritter A, Muñoz-Carpena R (2013) Performance evaluation of hydrological models: Statistical significance for reducing subjectivity in goodness-of-fit assessments. J. Hydrol. 2013, 480, 33–45. [CrossRef]

Silva SS, Brown F, Sampaio AO, Silva ALC, Rodrigues NCRS, Lima AC, ... & Fearnside PM (2023) Amazon climate extremes: Increasing droughts and floods in Brazil's state of Acre. *Perspectives in Ecology and Conservation*, 21, 311–317

Tang J, Li Y, Cui S, Xu L, Hu Y, Ding S, and Nitivattananon, V (2021) Analyzing the spatiotemporal dynamics of flood risk and its driving factors in a coastal watershed of southeastern China. Ecol. Indicat. 121, 107134. https://doi.org/10.1016/j.ecolind. 2020.107134

U.S. Army Corps of Engineers USACE (2010) HEC-RAS, River Analysis System Hydraulic Reference Manual, Version 4.1; Hydrologic Engineering Center (HEC): Davis, CA, USA, 2010

U.S. Army Corps of Engineers USACE (2010). *HEC-RAS, River Analysis System Hydraulic Reference Manual, Version 4.1*; Hydrologic Engineering Center (HEC): Davis, CA, USA, 2010

Van Alphen J, and Passchier R (2007) Atlas of Flood Maps, examples from 19 European countries, USA and Japen, Ministry of Transport, Public Works and Water Management, The Hague, Netherlands, prepared for EXCIMAP, available at: http://ec.europa.eu/ environment/water/flood risk/flood atlas/index.htm, 2007

Van der Sleen P, Decuyper M, Flores BM, Householder JE, & Holmgren M (2025) ENSO wildfires impact Amazonian floodplains in complex ways. *Ecosystems*, 28, 20

Vojtek M, Andrea P, Jana V, Shahla A (2019) Flood inundation mapping in small and ungauged basins: sensitivity analysis using the EBA4SUB and HEC-RAS modeling approach. *Hydrol. Res.* 2019, *50*, 1002–1019. https://doi.org/10.2166/nh.2019.163

Zhao G, Bates PD, Neal J, & Yamazaki D (2023) Flood defense standard estimation using machine learning and its representation in large-scale flood hazard modeling. *Water Resources Research*, 59, e2022WR032395. https://doi.org/10.1029/2022WR032395

FORMAÇÃO COMPLEMENTAR

2025-2025. Flooding Risk Assessment with Hec-Ras,Hec-HMS. (Carga horária: 7h).Udemy, UDEMY, Estados Unidos.

2024 – 2024. A Practical Introduction to 2D River Modelling in HEC-RAS (Carga horária: 9h) Udemy, UDEMY, Estados Unidos.

LISTA DE PUBLICAÇÕES
“PUBLISHED JOURNAL PAPERS”

1. BAIÃO, CHEILA FLÁVIA; MANTOVANI, JOSÉ; ALCÂNTARA, ENNER. Increasing Landslide Susceptibility in Urbanized Areas of Petrópolis Identified Through Spatio-Temporal Analysis. JOURNAL OF SOUTH AMERICAN EARTHSCIENCES

2. ALCÂNTARA, ENNER; BAIÃO, CHEILA FLÁVIA; GUIMARÃES, YASMIM CARVALHO; MANTOVANI, JOSÉ, ROBERTO; MARENGO, JOSE ANTONIO. Machine Learning Reveals Lithology and Soil as Critical Parameters in Landslide Susceptibility for Petrópolis (Rio de Janeiro State, Brazil). Natural Hazards Research, v. 4, p. 1, 2025.

3. **MANTOVANI, JOSÉ ROBERTO**; ALCÂNTARA, ENNER ;BAIÃO, CHEILA FLÁVIA ; PAMPUCH, LUANA ; CURTARELLI,MARCELO PEDROSO ; MARIANO RIBEIRO, JOÃO VITOR ;GUIMARÃES, YASMIM CARVALHO ; LONDE, LUCIANA ; MASSI,KLÉCIA ; MARENGO, JOSÉ ; NOBRE, CARLOS AFONSO ;ASSIREU, ARCILAN TREVENZOLI ; BORTOLOZO, CASSIANOANTONIO ; SIMÕES, SILVIO JORGE ; TOMASELLA, JAVIER ;LEAL DE MORAES, OSVALDO LUIZ ; PARK, EDWARD .Unprecedented Flooding in Porto Alegre Metropolitan Region (Southern Brazil) in May 2024: Causes, Risks and Impacts. JOURNAL OF SOUTH AMERICAN EARTH SCIENCES, v. 159, p.105533, 2025.

4. Mantovani, J. R., & Bueno, G. T. (2024). Mapping of planation surfaces in the north-central Amazonia. *Revista Brasileira De Geomorfologia*, *25*(4). https://doi.org/10.20502/rbg.v25i4.2554

5. Mantovani, J.; Alcântara, E.; Marengo, J.A.; Londe, L.; Park, E.; Cunha, A.P.; Tomasella, J. Flood Risk Mapping during the Extreme February 2021 Flood in the Juruá River, Western Brazilian Amazonia, State of Acre. *Sustainability* **2024**, *16*, 2999. https://doi.org/10.3390/su16072999

6. Marengo, J.A., Cunha, A.P., Seluchi, M.E. *et al.* Heavy rains and hydrogeological

disasters on February 18th–19th, 2023, in the city of São Sebastião, São Paulo, Brazil: from meteorological causes to early warnings. *Nat Hazards* **120**, 7997–8024 (2024). https://doi.org/10.1007/s11069-024-06558-5

7. Mantovani, J., Alcântara, E., Pampuch, L.A. *et al.* Assessing flood risks in the Taquari-Antas Basin (Southeast Brazil) during the September 2023 extreme rainfall surge. *npj Nat. Hazards* **1**, 9 (2024). https://doi.org/10.1038/s44304-024-00009-8

8. Mantovani J, R, Enner Alcântara, Thyago Anthony Soares Lima, Silvio Simões, An assessment of ground subsidence from rock salt mining in Maceio (Northeast Brazil) from 2019 to 2023 using remotely sensed data, Environmental Challenges, Volume 16, 2024, 100983, ISSN 2667-0100. https://doi.org/10.1016/j.envc.2024.100983.

9. Enner Alcântara, Cheila Flávia Baião, Yasmim Carvalho Guimarães, José Roberto Mantovani, José Antonio Marengo, Machine learning approaches for mapping and predicting landslide-prone areas in São Sebastião (Southeast Brazil), Natural Hazards Research, 2024, ISSN 2666-5921, https://doi.org/10.1016/j.nhres.2024.10.003. (https://www.sciencedirect.com/science/article/pii/S2666592124000751)

10. Enner Alcântara, Cheila Flávia Baião, Yasmim Carvalho Guimarães, José Antonio Marengo, José Roberto Mantovani, Climate Change-Induced Shifts in Landslide Susceptibility in São Sebastião (Southeastern Brazil), Natural Hazards Research, 2024, ISSN 2666-5921, https://doi.org/10.1016/j.nhres.2024.11.005. (https://www.sciencedirect.com/science/article/pii/S2666592124000921)

JOURNAL PAPERS UNDER REVIEW

Discover Geoscience: Decision on "Interpretable Machine Learning for Flood Susceptibility Mapping in the Metropolitan Region of São Paulo, Southeast Brazil".

Explainable AI Reveals Threshold-Based Flash Flood Drivers in the Guadalupe River Basin, Texas", which was submitted to npj Natural Hazards on 13 August 2025 UTC.

Journal: Geomatica
Title: Scale-Dependent Controls on Landslide Susceptibility in Angra dos Reis (Brazil) Revealed by Spatial Regression and Autocorrelation Analyses
Corresponding Author: Professor Enner Alcantara
Co-Authors: Ana Clara de Lara Maia; André Luiz dos Santos Monte Ayres; Cristhy Satie Kanai; Jamille da Silva Ferreira; Miguel Reis Fontes; Nathalia Moraes Desani; Yasmim Carvalho Guimarães; Cheila Flávia de Praga Baião; José Roberto Mantovani; Tulius Dias Nery; Jose A. Marengo

Manuscript Number: GEOMAT-D-25-00176
Ref: Submission ID 2cb31bfd-b311-4e2b-b0a1-d2ad2342b9c5

Please note that you are listed as a co-author on the manuscript "Interpretable Machine Learning for Flood Susceptibility Mapping in the Metropolitan Region of São Paulo, Southeast Brazil", which was submitted to Modeling Earth Systems and Environment on 10 May 2025 UTC.

If you have any queries related to this manuscript please contact the corresponding author, who is solely responsible for communicating with the journal.

Kind regards,

Editorial Assistant
Modeling Earth Systems and Environment

TRABALHOS COMPLETOS PUBLICADOS EM ANAIS DE CONGRESSOS

MANTOVANI, José Roberto; GUIMARÃES, Yasmim Carvalho; ALCÂNTARA, Enner Herenio de. FROM DATA TO DECISION: MULTI-CRITERIA MAPPING OF LANDSLIDE SUSCEPTIBILITY IN SÃO SEBASTIÃO. In: ANAIS DO XXI SIMPóSIO BRASILEIRO DE SENSORIAMENTO REMOTO, 2025, Salvador. Anais eletrônicos..., Galoá, 2025. Disponível em: <https://proceedings.science/sbsr-2025/papers/from-data-to-decision-multi-criteria-mapping-of-landslide-susceptibility-in-sao?lang=en> Acesso em: 14 Ago. 2025.

GUIMARÃES, Yasmim Carvalho et al. Geomorphological Factors Driving Flood Susceptibility In Recife: Identifying High-Risk Zones For Effective Mitigation. In: ANAIS DO XXI SIMPóSIO BRASILEIRO DE SENSORIAMENTO REMOTO, 2025, Salvador. Anais eletrônicos..., Galoá, 2025. Disponível em: <https://proceedings.science/sbsr-2025/papers/geomorphological-factors-driving-flood-susceptibility-in-recife-identifying-high?lang=en> Acesso em: 14 Ago. 2025.

COMPROVANTES E CERTIFICADOS

udemy

Nº do certificado: UC-559dd82f-0126-4457-a90d-34cc8d1cd4a1
URL do certificado: ude.my/UC-559dd82f-0126-4457-a90d-34cc8d1cd4a1
Número de referência: 0004

CERTIFICADO DE CONCLUSÃO

A Practical Introduction to 2D River Modelling in HEC-RAS

Instrutores **Nick Wallerstein**

José Roberto Mantovani

Data **20 de Agosto de 2024**
Duração **8.5 horas no total**

udemy

Nº do certificado: UC-b8effed1-266b-44d0-86be-5d9cbea25125
URL do certificado: ude.my/UC-b8effed1-266b-44d0-86be-5d9cbea25125
Número de referência: 0004

CERTIFICADO DE CONCLUSÃO

Flooding Risk Assessment with Hec-Ras, Hec-HMS, QGIS

Instrutores **Franck Diedro**

José Roberto Mantovani

Data **7 de Janeiro de 2025**
Duração **6.5 horas no total**

CERTIFICADO

SBSR
XXI SIMPÓSIO BRASILEIRO DE SENSORIAMENTO REMOTO

Certificamos que o trabalho intitulado

"Geomorphological Factors Driving Flood Susceptibility In Recife: Identifying High-Risk Zones For Effective Mitigation"

Yasmim Carvalho Guimarães, Andrés Velastegui-Montoya, Enner Herenio de Alcântara, José Roberto Amaro Mantovani

Apresentador(a): ***Yasmim Carvalho Guimarães***

foi apresentado no XXI Simpósio Brasileiro de Sensoriamento Remoto - SBSR, realizado no período de 13 a 16 de abril de 2025, em Salvador, BA.

Salvador, 16 de abril de 2025.

Lúbia Vinhas
Presidente Comitê Técnico-Científico

Luiz Eduardo Oliveira e Cruz de Aragão
Coordenador do SBSR

Marcos Adami
Coordenador de SBSR

Certification by Galoá

CERTIFICADO

SBSR
XXI SIMPÓSIO BRASILEIRO DE SENSORIAMENTO REMOTO

Certificamos que o trabalho intitulado

"FROM DATA TO DECISION: MULTI-CRITERIA MAPPING OF LANDSLIDE SUSCEPTIBILITY IN SÃO SEBASTIÃO"

José Roberto Mantovani, Yasmim Carvalho Guimarães, Enner Herenio de Alcântara

Apresentador(a): ***Yasmim Carvalho Guimarães***

foi apresentado no XXI Simpósio Brasileiro de Sensoriamento Remoto - SBSR, realizado no período de 13 a 16 de abril de 2025, em Salvador, BA.

Salvador, 16 de abril de 2025.

Lúbia Vinhas
Presidente Comitê Técnico-Científico

Luiz Eduardo Oliveira e Cruz de Aragão
Coordenador do SBSR

Marcos Adami
Coordenador de SBSR

Certification by Galoá

MINISTÉRIO DA EDUCAÇÃO
INSTITUTO FEDERAL FARROUPILHA
PRÓ-REITORIA DE PESQUISA, PÓS-GRADUAÇÃO E INOVAÇÃO

DECLARAÇÃO

Declaro, para fins de comprovação, que **José Roberto Amaro Mantovani** faz parte da Equipe de Revisores *ad hoc* da Revista de Ciência e Inovação (ISSN 2448-4091), do Instituto Federal Farroupilha, e realizou a avaliação do manuscrito nº 464, no ano de 2024.

Santa Maria, 20 de dezembro de 2024.

gov.br Documento assinado digitalmente
REJANE FLORES
Data: 20/12/2024 10:23:25-0300
Verifique em https://validar.iti.gov.br

REJANE FLORES

Editora-Chefe
Revista de Ciência e Inovação
Instituto Federal Farroupilha
Portaria nº 1231/2024

SPRINGER NATURE

REVIEWER CERTIFICATE

This certificate is awarded to

José Roberto Mantovani

in recognition of their contribution to

1 manuscript in 2025 for

Discover Geoscience

20 January 2025

Springer nature portfolio BMC Discover palgrave macmillan Birkhäuser Adis

SPRINGER NATURE

REVIEWER CERTIFICATE

This certificate is awarded to

José Roberto Mantovani

in recognition of their contribution to

2 manuscripts in 2025 for

Discover Geoscience

08 August 2025

Springer nature portfolio BMC Discover palgrave macmillan Birkhäuser Adis

Your review for Atmosphere has been added to your Web of Science researcher profile

Externa Caixa de entrada ×

Web of Science researcher profiles noreply@webofscience.com por amazonses.com
para mim

qua., 13 de ago., 22:01 (há 10 horas)

Clarivate™

Congratulations Jose Mantovani!

Your recent review of "Mechanistic Linkage Between Freeze-Thaw Cycles and Enhanced Erosion in Qinghai-Tibet Plateau Soils" for Atmosphere has automatically been added to your Web of Science researcher profile as part of our partnership with MDPI.

This review was added automatically because the automatic addition of reviews from partnered journals is enabled on your account. You can change this setting in your profile's review settings page. Please check our FAQ portal if you have any questions.

The review was added using your default privacy settings, although these may be subject to the official journal review policy. To see the details please of your review please view the review's edit page.

Got a question?
Check out our FAQs

Send review receipts to:
reviews@webofscience.com

Unsubscribe

Responder Encaminhar

Your review for Sustainability has been added to your Web of Science researcher profile

Externa Caixa de entrada ×

Web of Science researcher profiles noreply@webofscience.com por amazonses.com
para mim

qua., 16 de jul., 21:45

Traduzir para o português ×

Clarivate™

Congratulations Jose Mantovani!

Your recent review of "Dynamic Remote Sensing Monitoring and Analysis of Influencing Factors for Land Degradation in Datong Coalfield" for Sustainability has automatically been added to your Web of Science researcher profile as part of our partnership with MDPI.

This review was added automatically because the automatic addition of reviews from partnered journals is enabled on your account. You can change this setting in your profile's review settings page. Please check our FAQ portal if you have any questions.

The review was added using your default privacy settings, although these may be subject to the official journal review policy. To see the details please of your review please view the review's edit page.

Got a question?
Check out our FAQs

Send review receipts to:
reviews@webofscience.com

Unsubscribe

Your review for Remote Sensing has been added to your Web of Science researcher profile

Externa

Web of Science researcher profiles noreply@webofscience.com por amazonses.com
para mim

qui., 13 de fev., 23:16

Traduzir para o português ×

Clarivate™

Congratulations Jose Mantovani!

Your recent review of "Modelling a four decades hydrological pattern of a saline temporary lake by remote sensing techniques and meteorological data: Water cover area simulation under future climate change scenarios (RCP)." for Remote Sensing has automatically been added to your Web of Science researcher profile as part of our partnership with MDPI.

This review was added automatically because the automatic addition of reviews from partnered journals is enabled on your account. You can change this setting in your profile's review settings page. Please check our FAQ portal if you have any questions.

The review was added using your default privacy settings, although these may be subject to the official journal review policy. To see the details please of your review please view the review's edit page.

Got a question?
Check out our FAQs

Send review receipts to:
reviews@webofscience.com

Unsubscribe

Discover Geoscience: Thank you for your review on "Flood Mapping and Damage Assessment in the Sub-Lower Niger River Basin, Nigeria Using Cloud-Based Remote Sensing Tools" Externa Caixa de entrada ×

Discover Geoscience <discovergeoscience@springernature.com> sex., 8 de ago., 08:28 (há 6 dias)
para mim

Traduzir para o português

Ref: "Flood Mapping and Damage Assessment in the Sub-Lower Niger River Basin, Nigeria Using Cloud-Based Remote Sensing Tools"

Dear Dr José Roberto Mantovani,

Thank you for submitting your report to Discover Geoscience. We greatly value the time and effort you put into reviewing the manuscript.

We've attached a copy of the report for your reference. You can also use this email to verify your review activity with third party websites, such as Publons.

You can keep track of your reviewer work on the new Reviewer dashboard associated with your Springer Nature account, and download your certificates.

Please note that in order to download your certificate from the dashboard, the email address with which you submitted your review must be the same as your login / registered email to your Springer Nature account. You can update your email to an existing account, or register a new account if you don't already have one, using this link: https://my-profile.springernature.com

Thanks again for your review; we'll email you the decision on the manuscript as soon as it is made. Meanwhile, we hope that we can continue to benefit from your expertise in the future.

Kind regards,

Peer Review Advisors
Discover Geoscience

1 anexo • Verificados pelo Gmail

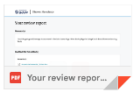

Responder Encaminhar

Your review for Engenharia Sanitaria E Ambiental has been added to Publons Caixa de entrada ×

Team Publons <noreply@publons.com> Cancelar inscrição dom., 20 de dez. de 2020, 17:34
para mim

Traduza para o português

publons

Congratulations José Mantovani!

Your recent review of "Validação de algoritmos de determinação da concentração de clorofila-a em um reservatório do semiárido brasileiro" for Engenharia Sanitaria E Ambiental has automatically been added to your Publons profile as part of our partnership with Associação Brasileira de Engenharia Santitária e Ambiental.

This review was added automatically because the automatic addition of reviews from partnered journals is enabled on your account. You can change this setting in your profile settings. Please check our FAQ portal if you have any questions.

The review was added using your default privacy settings, although these may be subject to the official journal review policy. To see the details of your review please view the status page.

Got a question?
Check out our FAQ

Send review receipts to:
reviews@publons.com

sustainability

Submit to this Journal

Review for this Journal

Propose a Special Issue

Article Menu

Academic Editor

Tommaso Caloiero

Subscribe SciFeed

Recommended Articles

Related Info Link

More by Authors Links

Order Article Reprints

Share Help Cite Discuss in SciProfiles

Open Access Article

Flood Risk Mapping during the Extreme February 2021 Flood in the Juruá River, Western Brazilian Amazonia, State of Acre

by José Mantovani [1,2], Enner Alcântara [1,2,*], José A. Marengo [2,3], Luciana Londe [2,3], Edward Park [4], Ana Paula Cunha [2,3] and Javier Tomasella [2,5]

[1] Institute of Science and Technology, São Paulo State University (Unesp), São José Dos Campos 12245-000, SP, Brazil

[2] Graduate Program in Natural Disasters, (Unesp/CEMADEN), São José Dos Campos 12247-004, SP, Brazil

[3] National Center for Monitoring and Early Warning of Natural Disasters (CEMADEN), São José Dos Campos 12247-016, SP, Brazil

[4] National Institute of Education, Earth Observatory of Singapore and Asian School of the Environment, Nanyang Technological University (NTU), Singapore 639798, Singapore

[5] National Institute for Space Research (INPE), Cachoeira Paulista 12630-000, SP, Brazil

* Author to whom correspondence should be addressed.

Sustainability **2024**, *16*(7), 2999; **https://doi.org/10.3390/su16072999**

Submission received: 1 March 2024 / Revised: 26 March 2024 / Accepted: 1 April 2024 / Published: 3 April 2024

(This article belongs to the Special Issue **Tropical Rivers and Wetlands: Impacts, Hazards, Conservation, and Management**)

Download Browse Figures Versions Notes

Abstract

Cruzeiro do Sul, a municipality in Northwestern Brazil is recurrently impacted by floods, particularly along the Juruá

Journal of South American Earth Sciences
Volume 160, July 2025, 105533

Unprecedented flooding in Porto Alegre Metropolitan Region (Southern Brazil) in May 2024: Causes, risks, and impacts

José Roberto Mantovani [a b], Enner Alcântara [a b], Cheila Flávia Baião [b], Luana Pampuch [a b], Marcelo Pedroso Curtarelli [c], João Vitor Mariano Ribeiro [b], Yasmim Carvalho Guimarães [b], Luciana Londe [b d], Klécia Massi [a b], José Marengo [b d], Carlos Afonso Nobre [b e], Arcilan Trevenzoli Assireu [f], Cassiano Antonio Bortolozo [d], Silvio Jorge Simões [b], Javier Tomasella [b g], Osvaldo Luiz Leal de Moraes [b], Edward Park [h]

https://doi.org/10.1016/j.jsames.2025.105533

Highlights

- A rare combination of El Niño and moisture transport corridors triggered record-breaking rainfall.
- Hydrodynamic flood modeling was calibrated using high-resolution topography and MERGE rainfall data.
- Land use change analysis (1985–2022) revealed increased urbanization and deforestation in flood-prone zones.
- Climate trend analysis using ETCCDI indices showed rising frequency of extreme rainfall events.

Heavy rains and hydrogeological disasters on February 18th–19th, 2023, in the city of São Sebastião, São Paulo, Brazil: from meteorological causes to early warnings

Original Paper | Published: 28 March 2024

Volume 120, pages 7997–8024, (2024) Cite this article

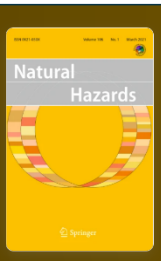

Natural Hazards

Aims and scope →

Submit manuscript →

Jose A. Marengo, Ana P. Cunha, Marcelo E. Seluchi, Pedro I. Camarinha, Giovanni Dolif, Vinicius B. Sperling, Enner H. Alcântara, Andrea M. Ramos, Marcio M. Andrade, Rodrigo A. Stabile, José Mantovani, Edward Park, Regina C. Alvala, Osvaldo L. Moraes, Carlos A. Nobre & Demerval Goncalves

Abstract

This study provides a thorough analysis of the landslides that occurred in the city of São Sebastião, on the northern coast of São Paulo state, Brazil, in February 18th–19th, 2023. The meteorological condition during this event was characterized by a cold front crossing over a warmer-than-normal subtropical South Atlantic, off the coast of São Paulo. Combined with the orographic effect of the Serra do Mar Mountain, the front remained stationary over the northern coastal areas of the state of São Paulo, causing an extreme and

npj | natural hazards

Article | Open access | Published: 03 June 2024

Assessing flood risks in the Taquari-Antas Basin (Southeast Brazil) during the September 2023 extreme rainfall surge

José Mantovani, Enner Alcântara ✉, Luana A. Pampuch, Cheila Flávia Praga Baião, Edward Park, Maria Souza Custódio, Luiz Felippe Gozzo & Cassiano Antonio Bortolozo

npj Natural Hazards **1**, Article number: 9 (2024) | Cite this article

Abstract

This analysis delves into precipitation dynamics in the Bacia Taquari Antas region, with a focus on September 2023. Employing a multi-scale approach encompassing monthly, daily, and subdaily analyses, the study unveils a consistent precipitation distribution throughout the year. September 2023's anomaly, the second-highest in the dataset, prompts investigation into potential climatic variability. Notably, the daily analysis highlights September 4th, 2023, as significant, emphasizing the importance of historical context in evaluating weather event severity. Subdaily scrutiny of September 4th reveals intense, localized precipitation, raising concerns about hydrological impacts such as flash floods. Positive trends in Rx5day (maximum consecutive 5-day precipitation amount) and R25 (number of days in a year when precipitation exceeds 25 mm) indices indicate an increase in heavy precipitation events, aligning with broader climate change concerns. Shifting focus to flood extent and impact assessment in the Taquari-Antas Basin, a simulation model depicts the temporal evolution of the flood, reaching its peak on September 4th. Examination of affected areas, rainfall volumes, and impacts on census sectors, cities, and buildings furnishes critical data for disaster management. This study contributes to localized precipitation comprehension and broader issues of climate trends,

ELSEVIER

Environmental Challenges

Volume 16, August 2024, 100983

An assessment of ground subsidence from rock salt mining in Maceió (Northeast Brazil) from 2019 to 2023 using remotely sensed data ☆

José Roberto Mantovani [a b], Enner Alcântara [a b], Thyago Anthony Soares Lima [a b], Silvio Simões [a b]

Show more

https://doi.org/10.1016/j.envc.2024.100983 ↗

Abstract

This study investigates ground subsidence in Maceió, the capital of Alagoas, Brazil, utilizing Sentinel-1 Synthetic Aperture Radar (SAR) data from November 2019 to December 2023. Ground subsidence poses significant risks to urban infrastructure and requires comprehensive monitoring and mitigation strategies. We employed the Interferometric Wide Swath (IW) mode of Sentinel-1A, acquiring high-resolution data in descending orbit with VV polarization. Through interferometric processing, including co-registration, phase unwrapping, and coherence estimation, we produced detailed subsidence maps for key neighborhoods such as Bebedouro, Farol, Mutange, Pinheiro, and Bom Parto. Our results reveal that subsidence in Maceió is highly variable across different neighborhoods, with cumulative subsidence reaching up to 3.83 meters in the most affected areas. The Bebedouro neighborhood, for instance, experienced subsidence up to 0.33 meters over an area of 41.85 hectares, while Farol saw significant ground movement impacting 59.49 hectares. The analysis indicates that high-density urban

KeAi CHINESE ROOTS GLOBAL IMPACT

Natural Hazards Research

Volume 5, Issue 2, June 2025, Pages 247-261

Machine learning approaches for mapping and predicting landslide-prone areas in São Sebastião (Southeast Brazil)

Enner Alcântara [a b], Cheila Flávia Baião [b], Yasmim Carvalho Guimarães [b], José Roberto Mantovani [b], José Antonio Marengo [b c]

Show more

https://doi.org/10.1016/j.nhres.2024.10.003 ↗

Abstract

This study employs machine learning techniques to map and predict landslide-prone areas in São Sebastião, Brazil, a region susceptible to landslides due to its steep terrain and intense rainfall. We compared five algorithms: Random Forest, Gradient Boosting, Support Vector Machine, Artificial Neural Network, and k-Nearest Neighbors, using various environmental factors as inputs. The Gradient Boosting model performed best, achieving an AUC-ROC of 0.963 and an accuracy of 99.6%. Slope degree, soil moisture index, and relief dissection emerged as the most influential factors in predicting landslide susceptibility. Analysis of land use and land cover changes between 1985 and 2021 revealed significant increases in forest cover and urban areas, with implications for landslide risk distribution. The resulting susceptibility map shows predominantly low-risk areas with scattered high-risk zones, providing crucial information for targeted risk management. This research demonstrates the effectiveness of machine learning in landslide susceptibility mapping and offers valuable insights for disaster risk reduction and urban planning in coastal mountainous regions.

KeAi CHINESE ROOTS GLOBAL IMPACT

Natural Hazards Research

Volume 5, Issue 2, June 2025, Pages 321-334

Climate change-induced shifts in landslide susceptibility in São Sebastião (southeastern Brazil)

Enner Alcântara [a b], Cheila Flávia Baião [b], Yasmim Carvalho Guimarães [b], José Antonio Marengo [b c d], José Roberto Mantovani [a b]

https://doi.org/10.1016/j.nhres.2024.11.005 ↗

Abstract

Landslides are a pressing natural hazard, particularly in regions prone to extreme weather events, and their frequency is expected to rise due to climate change. This paper investigates landslide susceptibility in São Sebastião, a coastal region in southeastern Brazil, under various climate change scenarios. The study fills a critical gap in understanding how future precipitation changes driven by climate models could affect the area's susceptibility to landslides. Current assessments often overlook the combined effects of environmental variables and land-use dynamics under future climate conditions. To bridge this gap, this research integrates environmental variables, including Soil Moisture Index (SMI), slope degree, saturation, relief dissection, geomorphology, geology, and topographic position index (TPI), with land use and land cover (LULC) data. Scenarios from the Intergovernmental Panel on Climate Change (IPCC) for RCP2.6, RCP4.5, RCP6.0, and RCP8.5 CMIP5 (Climate Models Intercomparison Programme Version 5) models were applied to model the impact of changing precipitation patterns on landslide susceptibility. Using geospatial data and a weighted sum model, susceptibility maps were

Peer-reviewed journal
e-ISSN: 2236-5664
REVISTA BRASILEIRA DE GEOMORFOLOGIA
Desde 2000
Since 2000
OPEN ACCESS

Mapping of planation surfaces in the north-central Amazonia

José Roberto Mantovani
Universidade Federal de Goiás
https://orcid.org/0000-0002-7051-5304

Guilherme Taitson Bueno
Universidade Federal de Goiás - Instituto de Estudos Sócio-Ambientais - IESA, Geografia, Goiás-GO, Brazil
https://orcid.org/0000-0003-4259-7354

DOI: https://doi.org/10.20502/rbg.v25i4.2554

Palavras-chave: Planation surfaces, Geoprocessing, Surface formations (Regoliths), Amazon

Resumo

This study aims to identify planation surfaces and their dissected reliefs in the Amazon, starting from the highlands of the border between Brazil, Venezuela and Guiana and ending near the axis of the Amazon River. Its connection with associated surface formations (regoliths) was also evaluated. The input data for the execution of the algorithm used were generated via geoprocessing techniques, which enabled the identification

PDF (English) Portuguese

Publicado
03-12-2024

Como Citar
Mantovani, J. R., & Bueno, G. T. . (2024). Mapping of planation surfaces in the north-central Amazonia. *Revista Brasileira De Geomorfologia*, *25*(4). https://doi.org/10.20502/rbg.v25i4.2554

Fomatos de Citação

Edição
v. 25 n. 4 (2024): OUT - DEZ

Seção
Artigos

KeAi
CHINESE ROOTS
GLOBAL IMPACT

Natural Hazards Research

Available online 14 January 2025

In Press, Journal Pre-proof What's this?

Machine Learning Reveals Lithology and Soil as Critical Parameters in Landslide Susceptibility for Petrópolis (Rio de Janeiro State, Brazil)

Enner Alcântara [1 2], Cheila Flávia Baião [2], Yasmim Carvalho Guimarães [2], José Roberto Mantovani [1 2], Jose Antonio Marengo [2 3 4]

Show more

https://doi.org/10.1016/j.nhres.2025.01.008 ↗

Abstract

Petrópolis, located in the mountainous region of Rio de Janeiro, Brazil, is frequently impacted by severe landslides, exacerbated by intense rainfall, steep topography, and unregulated urban growth. This study employs machine learning to assess and predict landslide susceptibility, integrating geological, hydrological, and anthropogenic factors. Five models—Random Forest, CatBoost, Support Vector Machine, Artificial Artificial Neural Network (ANN), and XGBoost—were evaluated, with CatBoost emerging as the optimal model (F1-score: 0.82; AUC-ROC: 0.88). Variable importance analysis revealed soil type and erodibility as critical soil parameters influencing susceptibility, alongside lithology, underscoring the significance of geological over purely topographic factors. These findings emphasize the utility of machine learning for landslide modeling, providing scalable methodologies applicable to similar geospatial risk assessments worldwide. Beyond local applications, this work offers actionable insights for urban planning and disaster risk management in mountainous urban regions.

Journal of South American Earth Sciences
Volume 160, July 2025, 105509

Increasing landslide susceptibility in urbanized areas of Petrópolis identified through spatio-temporal analysis

Cheila Flávia de Praga Baião [a b], José Mantovani [a b], Enner Alcântara [a b]

https://doi.org/10.1016/j.jsames.2025.105509

Highlights

- LR and MGWR combined to produce multiscale landslide susceptibility maps.
- Lithology and LULC contribute to increased landslide susceptibility.
- Forest cover and elevation reduce landslide susceptibility.
- Multitemporal analysis reveals an increase in high-susceptibility areas.
- Urban areas are almost entirely located in very high susceptibility zones.

Abstract

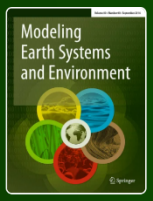

Modeling Earth Systems and Environment

Overview

The peer-reviewed journal Modeling Earth Systems and Environment (MESE) provides a unique publication platform by discussing interdisciplinary problems and approaches through modeling in earth and environment related fields, such as:

- Earth and environmental engineering; climate change; hydrogeology; aquatic systems and functions.
- Atmospheric research and water; land use and vegetation change; modeling of forest and agricultural dynamics; and economic and energy systems.
- Furthermore, the journal combines these topics with modeling of anthropogenic or social phenomena and projections to be used by decision makers.

Machine learning and climate scenario integration reveals controls on flood susceptibility in the Taquari-Antas Basin, Brazil

Original Article | Published: 08 September 2025
Volume 11, article number 410, (2025) Cite this article

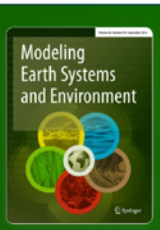

Enner Alcântara, Cheila Baião, Yasmim Guimarães & José Mantovani

Abstract

This study develops a comprehensive flood susceptibility assessment framework that integrates machine learning techniques with climate change scenarios in the Taquari River Basin, Southern Brazil. Using 23 environmental variables, including topographic, hydrological, and meteorological factors, the performance of five machine learning algorithms was evaluated. The Random Forest model demonstrated superior performance, achieving the highest accuracy (0.997) and ROC AUC (0.999) scores. Feature importance analysis revealed that the five-day maximum rainfall (14.25%), elevation (11.59%), and one-day maximum rainfall (10.39%) were the most influential predictors of flood

Geomatics Editorial Office <geomatics@mdpi.com>
para Enner, Ana, André, Cristhy, Jamille, Miguel, Nathalia, Yasmim, Cheila, mim, Tulius, Jose, Geomatics, Laurel

Dear Professor Alcântara,

Congratulations on the acceptance of your manuscript, and thank you for submitting your work to Geomatics. Please see the relevant manuscript details below:

Manuscript ID: geomatics-3833975
Type of manuscript: Article
Title: Scale-Dependent Controls on Landslide Susceptibility in Angra dos Reis (Brazil) Revealed by Spatial Regression and Autocorrelation Analyses
Authors: Ana Clara Lara Maia, André Luiz Santos Ayres, Cristhy Satie Kanai, Jamille Silva Ferreira, Miguel Reis Fontes, Nathalia Moraes Desani, Yasmim Carvalho Guimarães, Cheila Praga Baião, Jose Roberto Mantovani, Tulius Nery, Jose A Marengo, Enner Alcântara *
Received: 6 Aug 2025
E-mails: ac.maia@unesp.br, monte.ayres@unesp.br, cristhy.satie@unesp.br, jamille.ferreira@unesp.br, miguel.fontes@unesp.br, nathalia.desani@unesp.br, yasmim.guimaraes@unesp.br, cheila.baiao@unesp.br, j.mantovani@unesp.br, tulius.nery@cemaden.gov.br, jose.marengo@cemaden.gov.br, enner.alcantara@unesp.br